TÉCNICO LISBOA

Risk-based Ship Hull Hybrid Structural Design and Optimisation Employing Genetic Algorithm

Elios Koni

Thesis to obtain the Master of Science Degree in

Naval Architecture and Ocean Engineering

Supervisor: Prof. Yordan Garbatov

Examination Committee

Chairperson:	Prof. Ângelo Teixeira
Supervisor:	Prof. Yordan Garbatov
Committee Member:	Prof. Baiqiao Chen

October 2022

Acknowledgements

I would like to thank the coordinator of the MENO course, Prof. Ângelo Teixeira, for his contribution to developing a competitive and exciting master's degree and his help during the transition process.

My sincere gratitude goes to my supervisor, Prof. Yordan Garbatov, for accepting to be my advisor and for his continuous support in this very insightful yet challenging work.

Also, I would like to thank my colleagues at Técnico, a very important group of people who challenged me out of my comfort zone and helped me to grow as a student.

Last but not least, my family. Without their trustful support, little would I have achieved.

Abstract

The optimum ship hull design solution has always been a concern, and in recent years genetic algorithms to optimise the ship hull structure have been developed. The genetic algorithm's fundaments generate alternative solutions and compare them with pre-defined constants and objectives. The development of design solutions evolves through competition and controlled variations. Minimising the ship hull structure weight is essential in reducing the ship's capital (construction) expenditure and increasing the cargo capacity. The risk of the ship is associated with the loss of the ship, cargo, human life, environmental pollution, etc. It is a governing factor impacted by the chosen structural design solution and the measures taken to reduce the structural weight. The master's degree thesis employs a genetic algorithm to study the weight minimisation of a multi-purpose ship hull structure controlling the associated risk by accounting for several structural design variables. The risk and best design solution define the probability of compressive collapse of the stiffened plates and integral ship hull structure and the associated cost due to failure. The Pareto frontier solutions, calculated by the non-dominated sorting genetic algorithm, NSGA-II, will be employed to determine feasible solutions for the design variables. The first-order reliability method, FORM, will estimate the Beta reliability index based on the topology of the stiffened plates and ship hull structure as a part of the Pareto frontier solutions. The algorithm employed will not account for any manufacturing constraints and consequences due to the encountered optimal design solution.

Keywords: Structural design, ultimate bending capacity, first-order reliability methods, multi-objective optimisation, hybrid lightweight structures, honeycomb core sandwich construction

Resumo

A solução óptima de um projeto de casco de navio sempre foi uma preocupação, e nos últimos anos foram desenvolvidos algoritmos genéticos para optimizar a sua estrutura. Os algoritmos genéticos geram soluções alternativas e comparam-nas com constantes e objectivos pré-definidos. O desenvolvimento de soluções evolui através da comparação e variações controladas. A minimização do peso estrutural é essencial para reduzir o custo de capital (construção) do navio e para aumentar a capacidade de carga. O risco está associado à perda do navio, da carga, da vida humana, da poluição ambiental, etc. Sendo este um factor determinante, influenciado pela solução estrutural escolhida e pelas medidas tomadas para reduzir o peso estrutural. A tese de mestrado empregará um algoritmo genético para estudar a minimização do peso de uma estrutura de casco de navio multiuso, controlando o risco associado através da contabilização de várias variáveis do projecto estrutural. A probabilidade de colapso compressivo dos painéis enrijecidos, estrutura integral do casco do navio e o custo associado devido a falha é utilizada como base para definir o risco e a melhor solução. As soluções de fronteira de Pareto, calculadas pelo algoritmo genético de classificação não dominado, NSGA-II, serão utilizadas para determinar soluções viáveis. O método de fiabilidade de primeira ordem, FORM, estimará o índice de fiabilidade Beta com base na topologia das placas e da estrutura do casco como parte das soluções da fronteira de Pareto. O algoritmo utilizado não leva em consideração quaisquer restrições e consequências de fabrico devido à solução ideal encontrada.

Palavras Chave: Projeto estrutural, capacidade máxima de flexão, métodos de confiabilidade de primeira ordem, otimização multiobjetivo, estruturas leves híbridas, construção em sanduíche com núcleo hexagonal

Table of Contents

List of Figures

List of Tables

List of Abbreviations

ACO	Ant Colony Optimisation
AHS	Aluminium Honeycomb Structures
ALS	Accidental Limit State
BS	British Standards Institution
BV	Bureau Veritas
DNV	Det Norske Veritas
DWT	Deadweight Tonnage
EDW	Equivalent Design Wave
EEDI	Energy Efficiency Design Index
EMOO	Excel-based Multi-objective Optimisation
FEM	Finite Element Method
FEU	Forty-foot Equivalent Unit
FLS	Fatigue Limit State
FORM	First Order Reliability Method
FRP	Fiberglass Reinforced Plastic
FSA	Formal Safety Assessment
GA	Genetic Algorithm
IACS	International Association of Classification Societies
IMO	International Maritime Organization
ISM	International Safety Management
ISSC	International Ship and Offshore Structures Congress
ISUM	Idealised Structural Unit Method
LCFs	Load Combination Factors
LRFD	Load and Resistance Factor Design
LSD	Limit State Design
LW	Lightweight
MS	Microsoft
MSA	Maritime Safety Agency
NSGA	Non-dominated Sorting Genetic Algorithm
PSO	Particle Swarm Optimisation
QRA	Quantitative Risk Assessment
SLS	Serviceability Limit State
SOLAS	Safety of Life at Sea
TEU	Twenty-foot Equivalent Unit
ULS	Ultimate Limit State
VBA	Visual Basic for Applications
VCG	Vertical Centre of Gravity
VEGA	Vector Evaluated Genetic Algorithms

List of Symbols

A	Area
B	Breadth of the ship
b	Width of the panel
C_b	Block coefficient
C_{ship}	Capital cost of the ship
$\overline{C}_{Steel}$	Average cost of steel
C_W	Wave parameter
D	Depth of the ship
	Bending stiffness
E	Young's modulus
F	Objective function
$F_{1,0}$	Original ship's lightweight
$F_{2,0}$	Permissible stress of 390 MPa steel
G	Shear modulus
h	Distance between facing skin centres
	Weibull shape parameter
h_c	Honeycomb core height
	Height of the core
I_y	Inertial moment
I_{Ry}	Required inertial moment
k	Material factor
L	Length of the ship
M_{SW}	Still water bending moment
M_U	Ultimate bending moment
$M_{W,e}$	Extreme value of M_{WV}
M_{WV}	Wave-induced bending moment
n	Number of cycles
P	Applied load
p	Partial time in full-load seagoing conditions
P_f	Probability of failure
q	Uniformly distributed load
	Weibull scale parameter
R	Resistance
S	Load effect
s	Cell size
T	Draught
t_{eq}	Equivalent thickness
t_f	Thickness of facing skin
T_r	Reference time period
T_W	Average wave period
$W_{AHS,Steel}$	Weight per unit meter of the hybrid structure
W_{Steel}	Weigh per unit meter of the steel structure
x	Design variable
$\widetilde{x}_i$	Uncertainty factors
x^L	Lower bound of the design variable
x^U	Upper bound of the design variable
Z	(Geometrical) Modulus

z_n	Z coordinate of the horizontal neutral axis of the transverse hull section
α_m	Gumbel location parameter
β	Reliability index
β_m	Gumbel scale parameter
γ_R	Partial safety factor for the ultimate bending capacity
δ_{al}	Allowable deflection
ϵ	Strain
υ	Poisson's ratio
ρ	Density
σ_{al}	Allowable stress
σ_{perm}	Permissible stress
σ_y	Yield stress
χ	Curvature
$\%W_{AHS}$	Weight percentage of AHS structure per unit length

1 Introduction

Ship design is a complex process due to the considerable number of technical aspects; their optimisation may be very different in the distinct stages of design and result in conflicting solutions. Design tasks, such as main dimensions, hull form and resistance, general arrangement, propulsion, structure, stability and manoeuvrability, safety, production, etc., were initially performed with Sequential Engineering, described in (Evans, 1959) as a Design Spiral, made ship design process where multiple iterations achieved the pseudo-optimum solution. This peculiarity made Sequential Engineering time-consuming and costly.

With the development of recent technologies, many design tasks can be performed simultaneously, considering multiple technical aspects in the early design stages. This methodology, called Concurrent Engineering, has a positive impact on the optimisation of production, delivery time and, therefore, the costs along the ship's lifecycle, with an increased knowledge of the product at a preliminary stage.

The development of genetic algorithms (**GA**s) in recent years has contributed to the optimisation of the ship hull structure, with the possibility of integrating multiple criteria in the decision-making. Minimising the ship hull structural weight is essential in reducing the ship's capital (construction) expenditure and increasing the cargo capacity. The risk of the ship is associated with the loss of the ship, cargo, human life, environmental pollution, etc., a governing factor impacted by the chosen structural design solution and the measures taken to reduce the structural weight.

The advantage of **GA**s in ship hull structural optimisation is their ability to deal with highly non-linear problems. In this work, design variables, such as plate panel thicknesses, bulb profiles, span, aluminium honeycomb core density and materials, are discrete variables not dealt with in a standard linearisation approach involving gradients in the search process. Therefore, the complexity of this optimisation lies in translating the discrete nature of the design variables into a model, considering many constraints given by the Class Societies' Rules. With this respect, **GA**s allow obtaining a set of Pareto-optimum solutions which give a complete view of the problem, rather than applying classical approaches, among others: objective weighting, distance functions and min-max formulations (Srinivas, et al., 1994), to obtain a single point solution. The obtained Pareto-optimal front allows the decision maker to compare multiple solutions as a function of additional measures of merit, in this case, the β-reliability index.

The International Maritime Organization (IMO) target is to reduce greenhouse gas emissions from shipping by at least 50% in 2050 compared to 2008 plays a key role in the ship hull structural weight minimisation, considering that the maritime sector accounted for more than 3% of worldwide CO_2 emissions. Applying alternative design solutions, such as Aluminium Honeycomb Structures (AHS), may reduce the hazardous and polluting emissions throughout the ship's lifecycle (Nepomuceno de Oliveira, et al., 2022). Aluminium is a versatile and recyclable material (Mahfoud & Emade, 2010). It can contribute to fuel savings, power reduction, increased cargo capacity and improvement of the Energy Efficiency Design Index (EEDI) for new ships (IMO, 2011).

However, potential applications of AHS to strength parts of the structure, such as the inner shell, are still limited due to the incapacity of AHS to resist axial compressive loads generated by the vertical bending moment.

1.1 Motivation and Objective

The master's degree thesis will employ a genetic algorithm to study the weight minimisation of a multi-purpose hybrid ship hull structure controlling the associated risk by accounting for several structural design variables. The probability of compressive collapse of the stiffened plates, integral ship hull structure and the associated cost due to failure is used as a base to define the risk and best design solution. The Pareto frontier solutions, calculated by the non-dominated sorting genetic algorithm, NSGA-II, will be employed to determine feasible solutions for the design variables. The first-order reliability method, FORM, will estimate the Beta reliability index based on the topology of the stiffened plates and ship hull structure as a part of the Pareto frontier solutions. The algorithm employed will not account for any manufacturing constraints and consequences due to the encountered optimal design solution.

The scope of this work is to contribute to the analysis of the potential advantages of AHS in hybrid ship hull structures, given future developments in understanding the interaction between steel plate panels and AHS panels.

1.2 Structure

The master's degree thesis is organised into 5 Chapters:

- Chapter 1 briefly introduces the thesis and its context in the current state of design optimisation;
- Chapter 2 comprises the current state of the art of the several topics involved in the thesis, along with a historical background highlighting the significant developments;
- Chapter 3 describes the model the thesis is applied to and the multi-optimisation problem, identifying the objective functions, the design variables, and the constraints;
- Chapter 4 presents and discusses the results of the multi-optimisation problem, the ultimate strength associated with the Pareto-optimal solutions and their reliability;
- Chapter 5 draws conclusions from the work and proposes some undiscovered possible developments.

2 State of the Art

This chapter presents state of art, with a historical background highlighting the significant developments of the following topics: ship structural design, limit states design, reliability and risk-based design, lightweight structures, optimisation algorithms and structural optimisation.

2.1 Ship structural design

The development of innovative technologies over the past century has considerably impacted the maritime industry, ranging from developments in shipbuilding and ships to ship structural design.

Before the development of finite element methods (FEM), ship hull structures were designed and dimensioned with empirical methods solely based on classification societies' rules, which were themselves the result of accumulated experience and feedback from ships in service. New designs, therefore, were based on the designer's experience, similar to previous designs or a combination of both. These were finally checked against class rules and eventually sent-in in production. The limitations of an empirical method design approach can be identified in three main aspects:

a. Margin against failure remains unknown due to simplifications on failure modes and their interdependency;
b. Failure modes are numerous, and specific design solutions and a specific empirical formula may not cover considerations;
c. Simplifications in the empirical formulations imply limited applicability.

Based on this approach, the designer cannot quantify the influence of variables' change in a new design. Due to the missing functional link between input design variables and output design criteria, different variants cannot be analysed; therefore, the best design solution cannot be identified. This leads to a relevant probability of the criteria not being fulfilled in the best possible way.

The development of finite element methods and computers in the last 50 years introduced a consistent increase in analysis capacities, making it possible to move to a rationally-based design approach (Hughes, et al., 1980). This design approach is directly and entirely based on the structural theory and computer-based methods of structural analysis and optimisation in achieving an optimum defined structure based on designer-selected measures of merit.

Rationally-based design is not automated; therefore, decisions (objectives, properties, criteria, constraints…) must be made before the design process. However, the two design approaches are complementary and employed where most appropriate. The latter is mainly used in a preliminary ship design phase where the principal dimensions are determined by a given set of requirements and limitations. Based on these, the designer must determine the complete set of scantlings to provide adequate strength and safety for the least cost. On the other hand, empirical methods are particularly suitable for detail design, which is primarily guided and constrained by fabrication methods and requirements and, due to a large number of local structural components, can be implemented in mass production (Hughes & Paik, 2010; Palaversa, et al., 2020).

2.2 Limit states design

Limit State Design (LSD), also referred to as Load and Resistance Factor Design (LRFD), is a reliability-based design approach that was developed in the 1930s for use in the Civil Engineering industry (Brand, et al., 1995), describing a state beyond which a structure no longer satisfies the requirements. For marine structures, this is subdivided into four categories: Serviceability limit state (SLS), Ultimate limit state (ULS), Fatigue limit state (FLS) and Accidental limit state (ALS) (IACS, 2021).

An accurate assessment of a structure's ultimate strength is critical throughout a ship's life cycle. Still, in practice, its prediction is not a trivial task due to the possible occurrence of high plastic strain regions, tripping phenomena, residual stresses, imperfections, etc. Research in this field follows three principal areas: empirical, analytical, and numerical methods (ISSC, 2003).

An essential contribution to the analytical derivation of the hull's ultimate strength came from Caldwell (1965). He considered the buckling in compression and yielding in tension, also considering the change of the neutral axis in the section. Paik and Mansour (1995) proposed an analytical formulation that also considered double-hull cross-sections and material properties of various steel plates by adapting the original Caldwell formulation.

Smith (1977) introduced a progressive collapse method to estimate the longitudinal strength of a ship's hull, on which Paik (2003) elaborated a particular purpose computer program (ALPS/HULL) for the progressive collapse analysis until and after a ship hull reaches the ultimate strength, based on the Idealised Structural Unit Method (ISUM), developed by Ueda and Rashed (1984). This program is still in use today as a module of MAESTRO (MAESTRO Marine LLC Software).

Recent studies on the ultimate strength assessment have been conducted by Tekgoz et al. (2015) on a containership, accounting for the effect of neutral axis movement, translation, and rotation. The predicted ship's ultimate hull strength is compared to the solution of homemade software developed on the Common Structural Rules guidelines and finite element analysis performed by commercial software (ANSYS, 2012). Further studies on strength assessment were presented by Tekgoz and Garbatov (2020; 2021).

2.3 Reliability and risk-based design

Reliability aspects, intended as "the ability of an item to perform a required function, under given environmental and operational conditions, for a stated period", started to be considered in aeronautics in the 1930s, after World War I, with the collection of statistical data on the failure of various components and aircraft engines, initially expressed as a number of accidents per hour of flight time (Rausand, 1998). These data were further studied to improve the design and possibly avoid accidents—safety and reliability assessment techniques developed over the decades, mainly in aeronautical, aerospace and power industries. By the end of the 1970s was applied to a wide range of industries, from oil to railway and car industries (Wang, 1994).

The measure of reliability by use of a reliability β-index was introduced by Cornell (1969). Hasofer and Lind (1974) proposed a First-order Reliability Method (FORM) to calculate the β-index, of which the solution of the constrained optimisation problem can be solved iteratively with the Hasofer-Lind-Rackwitz-Fiessler algorithm (Rackwitz & Fiessler, 1978). Det Norske Veritas (DNV, 1992) contributed with a classification note on structural reliability analysis of marine structures.

Teixeira and Guedes Soares (2007a; 2007b) discussed how economic and social risk acceptance criteria have influenced the maritime industry, in particular by the implementation of safety measures onboard, and presented a cost-benefit and cost-effectiveness assessment of the optimal structural reliability of three tanker ships ranging from 230 to 313 m length.

Reliability analysis using a FORM has been employed to calculate the partial safety factors for a probability-based design rule of tankers to achieve pre-defined target safety levels. Results of this analysis were obtained for four tankers ranging from 133 to 313m in length (Teixeira & Guedes Soares, 2005). Parunov and Guedes Soares (2008) considered the ultimate collapse bending moment of a converted Aframax oil tanker to quantify the change in notion reliability levels applying the FORM. Feng et al. (2015) performed a reliability assessment (FORM) of three structural members of a bulk carrier on a direct strength calculation employing the von Mises stress failure criterion.

Reliability analysis, when extended to include the study of the consequences of the failures of the item in terms of possible damage to property, injury/death of people, and/or the degradation of the environment, is referred to as safety analysis (risk assessment), (Wang, et al., 2004).

Safety in the maritime industry became relevant after severe maritime accidents in the past century, including collisions, capsizes, oil spills and explosions of platforms. On this behalf, the first Safety of Human Life at Sea Convention (SOLAS) was adopted in 1914 in response to the Titanic disaster and is currently being replaced by SOLAS in 1974. The Geneva Convention (1948) established the International Maritime Organization (IMO), whose aims were summarised in art. 1. IMO developed a set of conventions, agreements and protocols dealing with various aspects of maritime safety, influencing the maritime industry to the risk and safety-oriented design. Among these, the fundamental international conventions are SOLAS (SOLAS, 1914-1974), Load Line Convention (1966), and Maritime Pollution Convention (MARPOL, 1973).

On the evidence of the investigation of the *Herald and Free Enterprise* capsize in 1993, the UK Maritime and Coastguard Agency (MSA) (MSA) proposed to IMO to apply Formal Safety Assessment (FSA) to ships, later introduced by IMO in 1997 (IMO, 1997; IMO, 2006; IMO, 2008; IMO, 2013). FSA was later modified and revised in 2018, defined as a structured and systematic methodology aimed at enhancing maritime safety, including protecting life, health, the maritime environment, and property (IMO, 2018).

On the evidence of the majority of shipping accidents being caused by human errors, estimated at approximately 80% (Guedes Soares & Teixeira, 2001), IMO has established an International Safety Management (ISM) Code, aiming at proving an international standard for the safe management and operation of ships and pollution prevention (IMO, 1993).

The need for a unified quantitative measure for safety in ships led to the development of Quantitative Risk Assessment (QRA) frameworks, first applied to Ro-Ro ferry safety in general by Spouge (1989). Two risk-assessment approaches are available: qualitative and quantitative risk assessment (Wang, 2006).

Wang et al. (1996) proposed an early application of QRA with a safety-based design and maintenance optimisation of large marine engineering systems applied to a hydraulic hoisting transmission system of a marine crane. Garbatov et al. (2018) proposed a risk-based framework for ship and structural design accounting for maintenance planning, composed of three consecutive stages, dealing with conceptual ship design, risk-based structural assessment and risk-based maintenance as a conclusion.

2.4 Lightweight structures

Structural weight saving may become particularly important in specific types of lightweight transportation, such as satellites, aircraft, high-speed trains, and fast ferries. The employment of sandwich structures over the increase of material thickness may be preferable. These structures are composed of two thin-facing layers separated by core material, providing excellent structural efficiency in a high strength-to-weight ratio (Paik, et al., 1999).

Depending on their application, the materials used for the manufacturing typically are steel, aluminium, thermoplastic polymers, Fiberglass Reinforced Plastic (FRP) and aramid paper, with various core configurations including corrugated core, honeycomb core, foam core, truss core and folded cores (Feng, et al., 2020).

Aluminium is a sustainable and versatile material due to its recyclability (Mahfoud & Emade, 2010). Therefore, the application of AHS could facilitate safe and environmentally reliable recycling of ships, as addressed by the Hong Kong International Convention (IMO, 2009), along with a variety of benefits concerning mechanical properties, fire safety, manufacturing accuracy and fabrication price (Kujala & Klanac, 2005).

These structures have been initially adopted for small vessels and, for bigger ships, non-strength parts of structures due to various problems in applying dynamically loaded structures (Paik, et al., 1999). The 1973

Pay'N Pak was the first (racing) boat built in AHS (Bitzer, 1994). Practical applications on larger vessels were realised from the 1990s onwards by the US Navy on antenna platforms and by the shipyard *Meyer Werft* on cruise ships (Kujala & Klanac, 2005). A more extensive application of sandwich structures finds a place in the 72m Visby class corvette by the Swedish Navy (Zenkert, et al., 2005).

Research on sandwich structures dates to the 1940s, dealing with the buckling of panels. Later, in the 1960s, the books of Plantema (1966) and Allen (1969) outlined the theory and analysis methodologies of sandwich structures, followed by the books of Zenkert (1993) and Vinson (1999) a few decades later. Simple theoretical expressions of the shear modulus of honeycomb sandwich cores have been derived by Kelsey (1958). Experimental studies on buckling strength characteristics of aluminium honeycomb sandwich panels in axial compression were undertaken by Yeh and Wu (1991). (Kobayashi, et al., 1994) studied the Elasto-Plastic bending behaviour of sandwich panels. Paik et al. (1999) investigated the strength characteristics of aluminium sandwich panels with aluminium honeycomb cores theoretically and experimentally, based on the so-called equivalent plate thickness method in which a honeycomb sandwich panel subjected to in-plane loads is approximately replaced by a single skin panel with equivalent plate thickness (Okuto, et al., 1991).

Potential advantages of sandwich panels include the ability of their core to absorb strain energy, making composite construction particularly suitable for slamming impact alleviation (Qin & Batra, 2009). However, despite their excellent mechanical response to different loading conditions (Palomba, et al., 2021), the critical aspect of composite sandwich structures regards the joint between sandwich panels and other metal components. One solution to this problem is to adhesively bond metal profiles to the composite structure in a prefabrication phase; this allows for welding the composite structure directly to the metal structure (Hentinen, et al., 1997). Kharghani and Guedes Soares tested a model of a composite-to-steel hybrid balcony overhang under shear and bending loads, outlining how the stiffness mismatch between the metal and composite part is one of the crucial parts in the structural design.

2.5 Optimisation algorithms

Over the years, various search and optimisation algorithms, also called metaheuristics, have been developed and can be classified into single-solution-based and population-based metaheuristic algorithms (Katoch, et al., 2021). The formers utilise a single candidate solution and improve this solution by using local search, which can be stuck in local optima, to name a few: simulated annealing (Kirpatrick, et al., 1983) (Glover & Laguna, 1997). On the other hand, population-based metaheuristics utilise multiple candidate solutions during the search process. A few examples: Genetic Algorithms (GA) (Holland, 1975), Vector-Evaluated Genetic Algorithms (VEGA) (Schaffer, 1985), Ant Colony Optimisation (ACO) (Dorigo, et al., 1991), Particle Swarm Optimisation (PSO) (Kennedy & Eberhart, 1995).

A genetic algorithm is a search and optimisation method that mimics evolutionary principles and chromosomal processing in natural genetics. **GA**s works iteratively by successively applying reproduction, crossover and mutation operators until a termination criterion is satisfied.

GAs came into play in the 1960s with Holland (1975); during the first years mainly practised by Holland and his students (De Jong, 1975; Goldberg, 1983). Concerning traditional methods, many of which scalarise the objective vector into a single objective, being highly weight-sensitive and demanding a pre-developed knowledge about the underlying problem, **GA**s show great applicability to complex optimisation problems for their ability to represent the set of solutions in a set of Pareto-optimal points. Indeed, in a typical multi-objective optimisation problem, one solution may not exist that's best (global minimum or maximum), and the suitability of one solution depends on several factors, including the designer's choice, problem environment, etc. (Srinivas, et al., 1994).

One of the problems with VEGA, as realised by Schaffler himself, is its bias towards some Pareto-optimal solutions. Later, Goldberg (1989) suggested a nondominated sorting procedure to overcome this weakness

of VEGA, an idea on which Srinivas et al. (1994) based the formulation of the Non-Dominated Sorting Genetic Algorithm (NSGA). Over the years, the main criticisms of the NSGA approach concerned three main aspects: its high computational complexity of non-dominated sorting (population needs to be sorted in every generation), its lack of elitism which can speed up the performance of the **GA** significantly, and the need for specifying the sharing parameter to ensure diversity in a population to get a wide variety of equivalent solutions. Deb et al. (2002) have formulated a Fast Elitist Non-Dominated Sorting GA for multi-objective optimisation (NSGA-II) based on these aspects.

Numerous studies show that **GA**s are a successful tool for practical problems in ship structural design and optimisation (Klanac & Jelovica, 2007) and are widely used nowadays. A useful multi-objective optimisation program employing **GA**s was developed by Sharma et al. (2012), who introduced an MS Excel-based Multi-Objective-Optimisation (EMOO) Program. Termination criteria were later employed in the design of shell-and-tube heat exchangers (Wong, et al., 2016).

2.6 Structural optimisation

The first formulation of a multi-objective optimisation problem, restricted to two objectives, was developed by Edgeworth (1881). The problem was formulated as: "*It is required to find a point (x y) such that, in whatever direction we take an infinitely small step, P and* Π *do not increase together, but that, while one increases, the other decreases"* where *P* and Π represent the utilities of the *X* and *Y* party respectively.

Pareto (1906) oppositely formulated the problem by extending it to *n*-objectives, assuming the ophelimity is not known a priori: "*Let x and y be the quantities of economic goods X and Y possessed by an individual. Assumed that there is no reason to take account of the order in which these foods are consumed, that is, consider the arrangements xy and yx to be identical […]".*

Since then, the first optimisation application to ships only appeared with Harlander (1960), dealing with least-weight plate-stiffener arrangements for two different loading conditions, a uniform axial load and a uniform lateral load. Studies on a combination of loads and the impact of longitudinal and frame spacing on weight and cost were conducted by his student in the 1960s-1970s. The implementation of computer optimisation problems was carried out later by Evans and Khoushy (1963) and Nowacki et al. (1970).

An important application of genetic algorithms for multi-objective ship structures optimisation found a place on a double-hull tanker with Okada and Neki (1992). Nobuwaka and Zhou (1996) developed a discrete optimisation of ship structures applied to a cargo ship with large hatch openings with **GA** and investigated the influences of the penalty coefficient, population size, crossover probability and mutation probability on results and convergence of the problem in terms of the construction cost, adopting an allowable stress design approach. Jastrzebski and Sekulski (2005) applied a **GA** to the structural optimisation in terms of the weight of a high-speed craft, considering a discrete set of scantlings for plates, bulb extrusions and T-bar extrusions. At this stage of development, optimisation problems only dealt with one objective function at a time, keeping the other parameters frozen.

The concept of Omni-optimisation was presented by Klanac and Jelovica (2007), who developed an algorithm capable of performing single and multi-objective optimisation. A comparative study on the hull weight and vertical centre of gravity (VCG) of a fast ferry is performed between the two optimisation problems. Rigo (2003) applied multi-objective optimisation to a cruise ship, intending to reduce the cost of production and the weight of the structure based on the LBR-5 software developed by Rigo (2001).

Ultimate limit states were considered in the work of Hughes et al. (2014), who applied the VEGA to optimise the cargo hold of double-hull tankers. The optimisation was run in terms of structural weight, safety, and fabrication cost, considering as constraint six failure criteria for stiffened panels and grillages and by employing ALPS/ULSAP to evaluate the limit states for each panel. One year later, Ma et al. (2015) employed

a PSO algorithm to optimise an isolated midship section of the same ship in terms of weight, safety and production cost and extended the analysis to the ultimate strength of the midship section.

All previous concepts presented in this state-of-the-art were implemented by Garbatov and Georgiev (2017) with a reliability-based optimisation. The authors proposed a multi-objective non-linear structural optimisation of a stiffened plate subjected to combined stochastic compressive loads, accounting for the design's ultimate strength and reliability-based constraints. Three years later, Garbatov and Huang (2020) extended the concept to ship structures by employing an NSGA-II to minimise the structural component net-section area, lateral deflection and fatigue damage, accounting for the local fatigue damage and ultimate global strength and mapping the Pareto frontier solutions with a first-order reliability method.

3 Application to a multi-purpose ship

The ship object of optimisation is a 9,800 DWT multi-purpose ship class 100 A1, equipped for the carriage of containers, strengthened for heavy cargoes, ice class 1D, with the following main characteristics (Table 1):

Table 1. Ship main dimensions.

Property	Symbol	Value	Unit
Rule length	L	115.07	m
Breadth moulded	B	20.00	m
Depth moulded	D	10.40	m
Draught (scantling)	T	8.30	m
Block coefficient	C_B	0.719	

Transversally, the midship section can host no. 4 tiers and no. 6 rows of containers in both holds and covers, with a stacked weight of 100 t (TEU) or 120 t (FEU) in holds and a limited stack weight of 30 t (TEU) or 40 t (FEU) on covers.

3.1 Model

This section relates to the description of the multi-purpose ship's structure and the considered load cases in strength assessment. Loads, hull girder strength and local hull scantling are determined according to DNV rules for the classification of ships (DNV, 2021). Additional steel sandwich panel construction requirements can be found in DNV-CG-0154 (2021). Buckling check of steel structures is performed according to DNV rules for the classification of ships with a length of 100 metres and above (DNV, 2009). Design and buckling check of the honeycomb core sandwich panels is performed according to the Hexcel Composites manufacturer guide (HexCel Composites, 2000). The original steel structure model is shown in Figure 1. The nodes indicate the extensions of the plate panels.

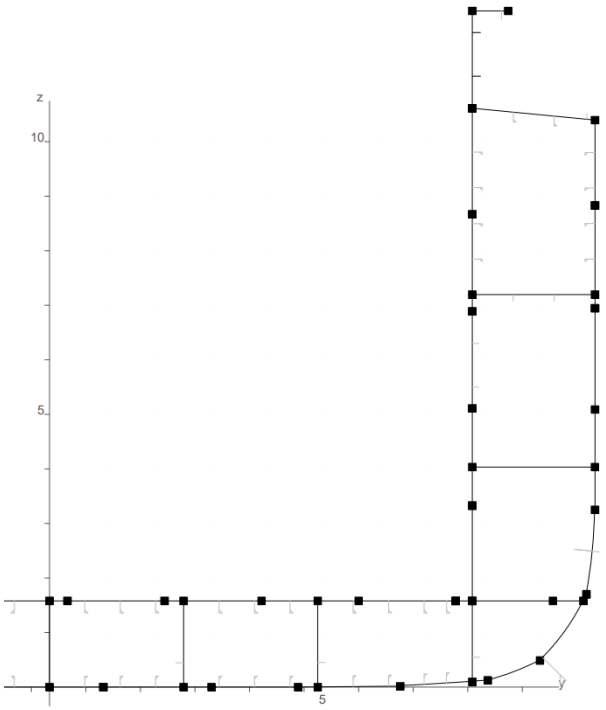

Figure 1. Half view of the original midship section.

3.1.1 Materials

The hybrid structure is composed of standard shipbuilding steels with a yield strength from 235 to 390 MPa, and AHS of aluminium alloy 5251-T3, replacing the vertical inner skin of the cargo hold. The material properties of steel and aluminium are shown in Table 2.

Table 2. Assumed properties of structural materials.

Property	Symbol	Value	Unit
Steel yield stress	$\sigma_{y,s}$	$235 - 390$	$\mathrm{N/mm^2}$
Steel Young's modulus	E_s	$2.05 \cdot 10^5$	$\mathrm{N/mm^2}$
Poisson's ratio	v	0.33	-
Steel density	ρ_s	7.8	t/m^3
Aluminium yield stress	$\sigma_{y,\,al}$	235	$\mathrm{N/mm^2}$
Aluminium Young modulus	E_s	$7.05 \cdot 10^4$	$\mathrm{N/mm^2}$
Aluminium density	ρ_{al}	2.7	t/m^3

The contribution of the honeycomb sandwich panels to strength calculations is considered with an equivalent single plate approach, in which the honeycomb sandwich panel is replaced by an equivalent single skin panel (Paik, et al., 1999), as summarised in Figure 2. This is performed by applying an equivalent rigidity method where in-plane tension, bending and shear are considered separately:

- In tension:

$$2t_f E_f = t_{eq,0} E_{eq} \tag{1}$$

- In bending:

$$\frac{1}{12}\left[\left(h_c + 2t_f\right)^3 - h_c^3\right] E_f = \frac{1}{12} t_{eq,0}^3 E_{eq} \tag{2}$$

- In shear:

$$2t_f G_f = t_{eq,0} G_{eq} \tag{3}$$

The equivalent single skin panel thickness $t_{eq,0}$ is obtained by solving the above equations, yielding:

$$t_{eq,\,0} = \sqrt{3h_c^2 + 6h_c t_f + 4t_f^2} \tag{4}$$

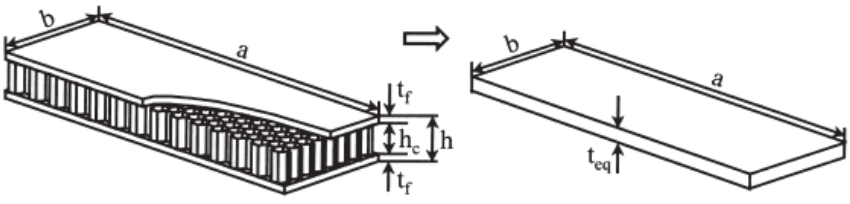

Figure 2. Equivalent single skin panel approach (Paik, et al., 1999).

The equivalent single-skin panels are later transformed to obtain a midship section composed of homogeneous materials. By defining the ratio $\mathrm{T} = E_{al}/E_s$ between Young's modulus of aluminium and steel, the new equivalent thickness is found by Eq. (5):

$$t_{eq} = \mathrm{T} \cdot t_{eq,0} \tag{5}$$

3.1.2 Load cases

The strength assessment is performed based on the combination of static plus dynamic load cases for complete load conditions at a probability level of 10^{-8}. The considered equivalent design waves (EDWs) to generate wave-induced dynamic load cases for structural assessment are HSM-2 and FSM-2, which maximise the vertical wave bending moment amidships for the head and following seas, respectively. The load combination factors (LCFs) are defined accordingly.

3.2 Structural optimisation

The multi-objective optimisation problem involves $\mathrm{K} \geq 1$ criteria and can be formulated as (Parsons & Scott, 2004; Sharma, et al., 2012):

$$\begin{cases} \min\limits_{\boldsymbol{x}} \ \mathrm{F}_1(\boldsymbol{x}) = [f_1(\boldsymbol{x}), f_2(\boldsymbol{x}), f_3(\boldsymbol{x}), \dots, f_K(\boldsymbol{x})] \\ \max\limits_{\boldsymbol{x}} \ \mathrm{F}_2(\boldsymbol{x}) = [f_1(\boldsymbol{x}), f_2(\boldsymbol{x}), f_3(\boldsymbol{x}), \dots, f_K(\boldsymbol{x})] \end{cases} \tag{6}$$

$$\boldsymbol{x} = [x_1, x_2, \dots, x_N]^T \tag{7}$$

Subject to the bounds on design variables and equality and inequality constraints:

$$\boldsymbol{x}^{\mathrm{L}} \leq \mathbf{x} \leq \mathbf{x}^{\mathrm{U}} \tag{8}$$

$$h_i(\boldsymbol{x}) = 0, \quad \mathrm{i} = 1, \dots, \mathrm{I} \tag{9}$$

$$g_i(\boldsymbol{x}) \geq 0, \quad \mathrm{j} = 1, \dots, \mathrm{J} \tag{10}$$

Where there are now K multiple optimisation criteria $f_1(\boldsymbol{x})$ through $f_K(\boldsymbol{x})$ and each depends on the N unknown design parameters in the vector $\boldsymbol{x}$. The overall cost function $\boldsymbol{F}$ is a vector. This problem generally has no single solution due to conflicts that typically exist among the K optimisation criteria.

When conflicting multiple criteria are present, the most common definition of an optimum is Pareto optimality (Pareto, 1906), for which "*A point is Pareto optimal if it satisfied the constraints and is such that no criterion can be further improved without causing at least one of the other criteria to decline".*

Note that this emphasises the conflicting or competitive interaction among the criteria. A point is weakly Pareto optimal if it satisfies the constraints and one criterion remains constant while at least one of the other criteria declines. These definitions typically result in a set of optimal solutions rather than a single unique solution. A design team typically seeks a single result that is a practical compromise or trade-off among the conflicting criteria.

Structural optimisation involves the interaction of multiple sub-processes interconnected together with the use of VBA. In the first stage, a ship's model is made as a function of the selected design variables, with complete information about midship sectional properties, loads, scantlings and buckling. This model was later integrated into the MS Excel MOO developed by Sharma et al. (2012) and Wong et al. (2016). Finally, the solutions are exported to MARS 2000 for ultimate strength calculation, and the Pareto-optimal front is mapped with the FORM. This automation process is divided into a first part dealing with the optimisation itself (Figure 3) and a second part dealing with the β-reliability index (Figure 4). Details about the flow chart involved in the MS Excel MOO program can be found in Sharma et al. (2017).

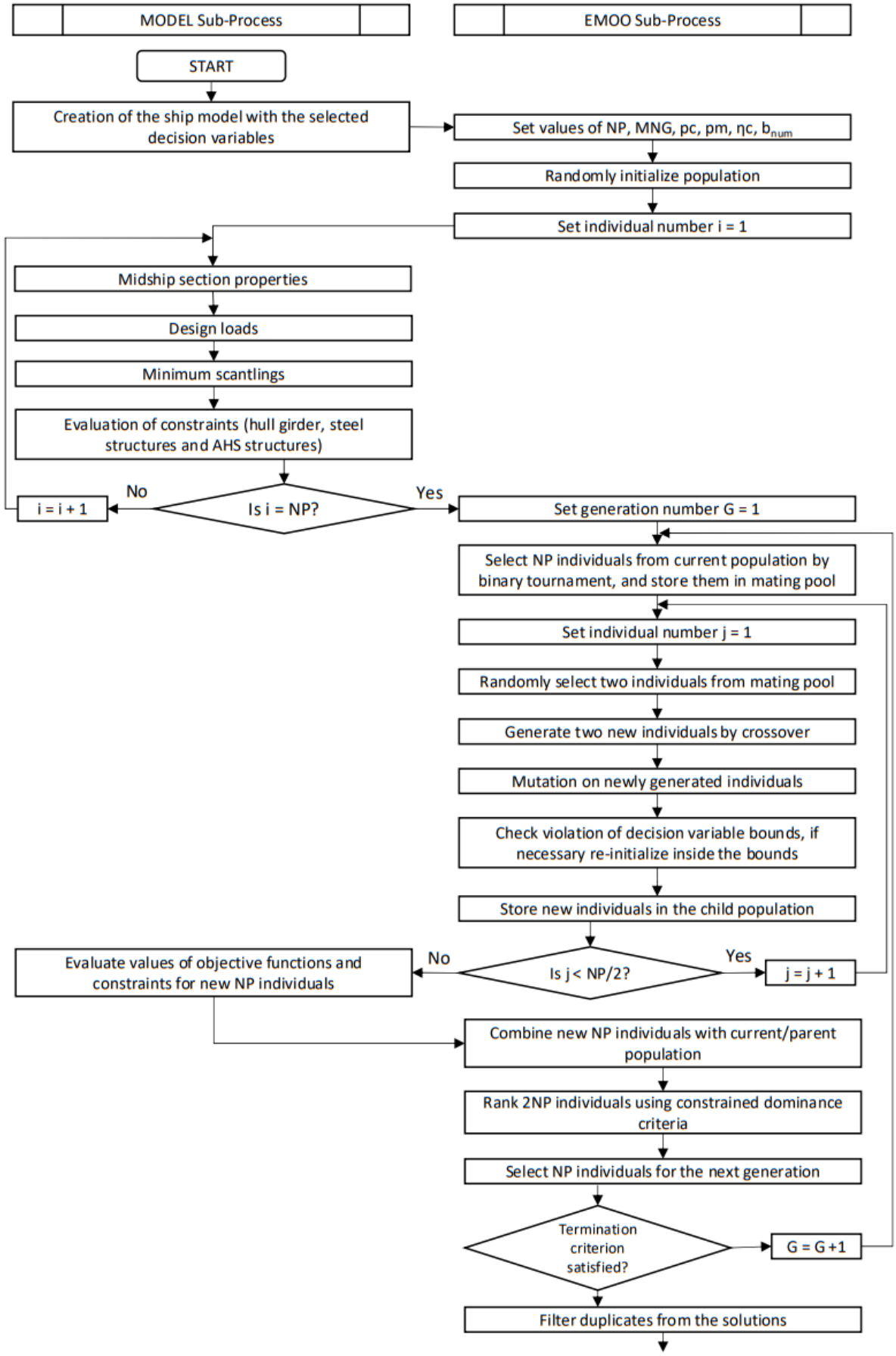

Figure 3. Optimisation Sub-process flowchart.

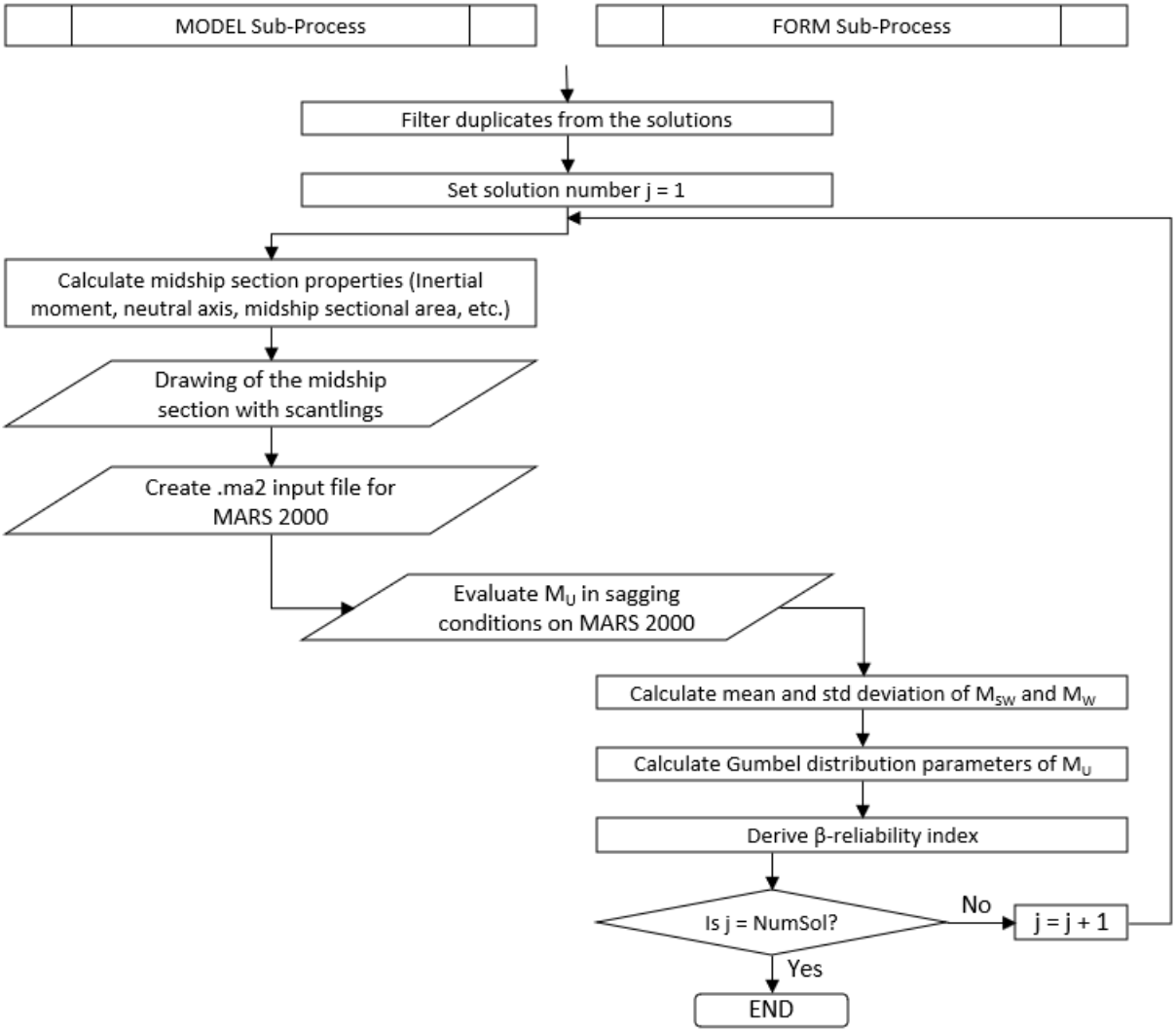

Figure 4. Reliability Sub-process flowchart.

3.2.1 Objective functions

The identified objective functions in the multi-optimisation problem relate to the ship's lightweight (LW), F_1 and the yield stress at the deck for sagging in seagoing conditions, F_2.

The regression formula can obtain the lightweight of the ship, as proposed in (Garbatov, et al., 2022):

$$\mathrm{LW} = 0.034 L^{1.7} B^{0.7} D^{0.4} C_B^{0.5} \left(0.2 + 0.8 \frac{W_{AHS,Steel}}{W_{Steel}}\right) \tag{11}$$

The longitudinal stress at the deck in sagging conditions, induced by still water and dynamic vertical hull girder bending, can be obtained by:

$$\sigma_d = \frac{M_{sw-s} + M_{wv}}{I_y} (z_d - z_n) \tag{12}$$

Where M_{sw-s} is the permissible vertical still water bending moment for sagging in seagoing conditions, M_{wv} is the vertical wave bending moment for the considered dynamic load case, I_y is the net moment of inertia

of the midship section about its horizontal neutral axis, z_d is the considered coordinate at the deck and z_n is the coordinate of the horizontal neutral axis about the keel.

3.2.2 Design Variables

In this optimisation problem, fifty-eight discrete design variables (Table 3-Table 4) have been identified to describe the midship section fully and can be divided into seven categories:

i. Ship hull gross plate thicknesses t_i
ii. Sandwich panel gross thicknesses $t_{pan,i}$;
iii. Sandwich plate gross thicknesses $t_{al,i}$;
iv. Steel bulb extrusions (Corus Special Profiles, 2002);
v. Span of the longitudinal members;
vi. Yield stress of steel;
vii. Cell density of sandwich panels' core.

The properties related to the design variables are listed in Tables Table 5Table 7. Choosing appropriate bounds on the design variables is crucial to facilitate the search algorithm. Selection of lower and upper bounds may be performed based on experience and/or minimum requirements.

The lower bound of steel and aluminium plate is determined by the minimum thickness requirements given by the rules, whereas the upper bound is set considering the type of the ship. Exception on the lower bound is made for variables $x_{14} - x_{17}$, where the minimum thickness is considered suitable for regular use of grabs of up to 10 tonnes of unladen weight, as indicated in the original midship section. Guidelines on AHS scantling are further given by DNV guidelines (DNV-CG-0154, 2021).

It is assumed that each stiffened plate panel is composed of homogeneous stiffeners. This is obtained by considering only the most loaded stiffener of each group to meet minimum scantling requirements and extend the scantling to the rest of the stiffeners. On the other hand, the buckling check follows the same rule, considering that the most loaded stiffener may not coincide with the most critical buckling-related condition.

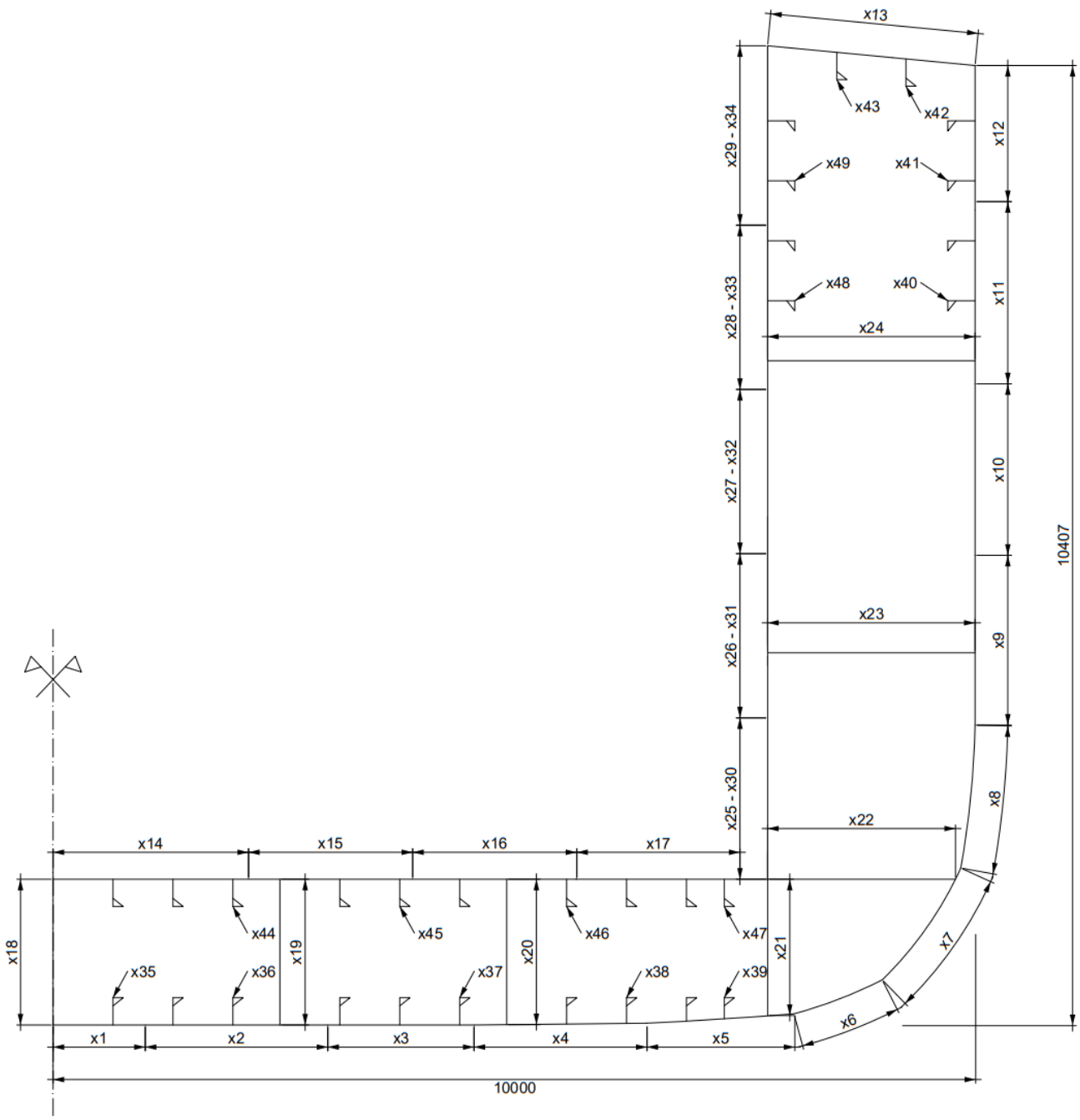

Figure 5. Representation of the design variables in the midship section.

Table 3. Design variables and their description (steel plates and sandwich structures).

Item	Symbol	Description	x^L mm	x^U mm	x_{step} mm
Steel plates	x_1	Bilge plate	11.5	18	0.5
	x_2	Bottom plate no. 1	10	18	0.5
	x_3	Bottom plate no. 2	10	18	0.5
	x_4	Bottom plate no. 3	10	18	0.5
	x_5	Bottom plate no. 4	10	18	0.5
	x_6	Bilge plate no. 1	10	22	0.5
	x_7	Bilge plate no. 2	10	22	0.5
	x_8	Side shell plate no. 1	9.5	18	0.5
	x_9	Side shell plate no. 2	9.5	18	0.5
	x_{10}	Side shell plate no. 3	9.5	18	0.5
	x_{11}	Side shell plate no. 4	9.5	18	0.5
	x_{12}	Side shell plate no. 5	9.5	20	0.5
	x_{13}	Deck plate no. 1	8	20	0.5
	x_{14}	Inner bottom plate no. 1	15	18	0.5
	x_{15}	Inner bottom plate no. 2	15	18	0.5
	x_{16}	Inner bottom plate no. 3	15	18	0.5
	x_{17}	Inner bottom plate no. 4	15	18	0.5
	x_{18}	Central girder panel	8	18	0.5
	x_{19}	Side girder panel no. 1	8	18	0.5
	x_{20}	Side girder panel no. 2	8	18	0.5
	x_{21}	Side girder panel no. 3	8	18	0.5
	x_{22}	Lower stringer panel	7.5	18	0.5
	x_{23}	Middle stringer panel	7.5	18	0.5
	x_{24}	Upper stringer panel	7.5	18	0.5
Sandwich Panels	x_{25}	Inner skin panel no. 1	20	60	0.5
	x_{26}	Inner skin panel no. 2	20	60	0.5
	x_{27}	Inner skin panel no. 3	20	60	0.5
	x_{28}	Inner skin panel no. 4	20	60	0.5
	x_{29}	Inner skin panel no. 5	20	60	0.5
Sandwich Plates	x_{30}	Inner skin plate no. 1	5.5	10	0.5
	x_{31}	Inner skin plate no. 2	5.5	10	0.5
	x_{32}	Inner skin plate no. 3	5.5	10	0.5
	x_{33}	Inner skin plate no. 4	5.5	10	0.5
	x_{34}	Inner skin plate no. 5	5.5	10	0.5

Table 4. Design variables and their description (stiffeners, span, yields stress and cell density).

Item	Symbol	Description	x^L	x^U	x_{step}
Stiffeners	x_{35}	Keel stiffener	1	59	1
	x_{36}	Bottom stiffener no. 1	1	59	1
	x_{37}	Bottom stiffener no. 2	1	59	1
	x_{38}	Bottom stiffener no. 3	1	59	1
	x_{39}	Bottom stiffener no. 4	1	59	1
	x_{40}	Side shell stiffener no. 1	1	59	1
	x_{41}	Side shell stiffener no. 2	1	59	1
	x_{42}	Deck stiffener no. 1	1	59	1
	x_{43}	Deck stiffener no. 2	1	59	1
	x_{44}	Inner bottom stiffener no. 1	1	59	1
	x_{45}	Inner bottom stiffener no. 2	1	59	1
	x_{46}	Inner bottom stiffener no. 3	1	59	1
	x_{47}	Inner bottom stiffener no. 4	1	59	1
	x_{48}	Inner skin stiffener no. 1	1	59	1
	x_{49}	Inner skin stiffener no. 2	1	59	1
Span	x_{50}	Multiple stiffeners' spacing	3	5	1
Yield stress	x_{51}	Lower section	1	4	1
	x_{52}	Middle section	1	4	1
	x_{53}	Upper section	1	4	1
Core cell density	x_{54}	Inner skin panel no. 1	1	7	1
	x_{55}	Inner skin panel no. 2	1	7	1
	x_{56}	Inner skin panel no. 3	1	7	1
	x_{57}	Inner skin panel no. 4	1	7	1
	x_{58}	Inner skin panel no. 1	1	7	1

Table 5. Steel yield stresses and related factors from DNV (2021).

Item	R_{eH} $\mathrm{N/mm^2}$	k	f
1	235	1.00	1.00
2	315	0.78	1.28
3	355	0.72	1.39
4	390	0.66	1.47

Table 6. Geometric properties of bulb flats (Corus Special Profiles, 2002).

Item	Bulb flat	Area cm^2	Item	Bulb flat	Area cm^2	Item	Bulb flat	Area cm^2
1	120 x 6	9.31	21	220 x 10	29.00	41	320 x 13	57.40
2	120 x 7	10.50	22	200 x 12	29.60	42	340 x 12	58.80
3	120 x 8	11.70	23	220 x 11	31.20	43	320 x 14	60.60
4	140 x 6.5	11.70	24	240 x 9.5	31.20	44	340 x 13	62.20
5	140 x 7	12.40	25	240 x 10	32.40	45	340 x 14	65.50
6	140 x 8	13.80	26	220 x 12	33.40	46	370 x 12.5	67.80
7	160 x 7	14.60	27	240 x 11	34.90	47	340 x 15	69.00
8	160 x 8	16.20	28	260 x 10	36.10	48	370 x 13	69.60
9	140 x 10	16.60	29	240 x 12	37.30	49	370 x 14	73.30
10	160 x 9	17.80	30	260 x 11	38.70	50	370 x 15	77.00
11	180 x 8	18.90	31	280 x 10.5	41.20	51	400 x 13	77.40
12	180 x 9	20.70	32	260 x 12	41.30	52	370 x 16	80.70
13	160 x 11.5	21.80	33	280 x 11	42.60	53	400 x 14	81.40
14	180 x 10	22.50	34	280 x 12	45.50	54	400 x 15	85.40
15	200 x 8.5	22.60	35	300 x 11	46.70	55	400 x 16	89.40
16	200 x 9	23.60	36	280 x 13	48.40	56	430 x 14	89.70
17	180 x 11.5	25.20	37	300 x 12	49.70	57	430 x 15	94.10
18	200 x 10	25.60	38	320 x 11.5	52.60	58	430 x 17	103.00
19	220 x 9	26.80	39	300 x 13	52.80	59	430 x 20	115.00
20	200 x 11	27.60	40	320 x 12	54.20			

Table 7. Mechanical properties of honeycomb core (HexCel Composites, 2000).

					Plate Shear			
Product Construction			Compression		L Direction		W Direction	
Item	Density kg/m^3	Cell size in	Strength N/mm^2	Modulus N/mm^2	Strength N/mm^2	Modulus N/mm^2	Strength N/mm^2	Modulus N/mm^2
1	37	0.25	1.4	310	1.0	220	0.6	112
2	50	0.19	2.3	517	1.5	310	0.9	152
3	54	0.25	2.6	620	1.6	345	1.1	166
4	72	0.13	4.2	1034	2.3	483	1.5	214
5	83	0.25	5.2	1310	2.8	565	1.8	245
6	127	0.25	10.0	2345	4.8	896	2.9	364
7	130	0.13	11.0	2414	5.0	930	3.0	372

3.2.3 Constraints

The applicable constraints to the optimisation problem can be divided into three sets of constraints: hull girder, steel structures and AHS. Additionally, constraints on the coefficients introduced in AHS have been set to meet their domain of definition. The total number of identified constraints amounts to 167.

3.2.3.1 Hull girder constraints

The constraints applicable to the hull girder are connected to the midship section and may be summarised as follows:

i. Inertial moment:

$$I_y - I_{Ry} \geq 0 \tag{13}$$

where:

$$I_{Ry} = 3 f_r C_W L^3 \mathrm{B}(C_B + 0.7) \tag{14}$$

ii. Modulus at bottom

$$Z_B - I_{Ry}/z_n \geq 0 \tag{15}$$

iii. Modulus at deck

$$Z_D - I_{Ry}/(D - z_n) \geq 0 \tag{16}$$

iv. Hull girder stress at bottom

$$\sigma_{al-b} - \frac{\max[(M_{sw-h} + M_{wv})\,;\ -(M_{sw-s} + M_{wv})]}{I_y} \cdot z_n \geq 0 \tag{17}$$

where σ_{al} is the allowable stress:

$$\sigma_{al-b} = 205/k_b \tag{18}$$

v. Hull girder stress at deck

$$\sigma_{al-d} - \frac{\max[(M_{sw-h} + M_{wv})\,;\ -(\mathrm{M}_{sw-s} + M_{wv})]}{I_y} \cdot (D - z_n) \geq 0 \tag{19}$$

where:

$$\sigma_{al-d} = 205/k_d \tag{20}$$

3.2.3.2 Constraints for steel structures

The set of constraints hereby listed relate to local scantling and buckling:

i. Minimum panel plate thickness:

$$t_i - t_{min} \geq 0 \tag{21}$$

ii. Minimum sectional area of bulb profile:

$$\mathrm{a} - 0.68\sqrt[3]{Z_{min}^2} \geq 0 \tag{22}$$

iii. Minimum bilge thickness concerning adjacent plates:

$$\min(x_6, x_7) - \max(x_5, x_8) \geq 0 \tag{23}$$

iv. Minimum critical buckling stress σ_c:

$$\sigma_c - \frac{\sigma_{al}}{\eta} \geq 0 \tag{24}$$

where σ_{al} is the compressive stress in plate panels, defined as:

$$\sigma_{al} = \frac{M_{SW} + M_{WV}}{I_y}(z_n - z_a) \tag{25}$$

Where z_a is the vertical distance from the baseline or deckline to the point in question below or above the neutral axis, respectively, z_n is the vertical distance from the baseline or decline to the neutral axis of the hull girder, whichever is relevant.

3.2.3.3 Constraints for AHS structures

The constraints applicable to AHS relate to simply supported plate and end load conditions. The constraints applicable to simply supported plates may be summarised in Equations 26-30, whereas constraints relating to end load conditions are given in Equations 31-36.

i. Minimum sectional area of bulb profile:

$$\mathrm{a} - 0.68\sqrt[3]{Z_{min}^2} \geq 0 \tag{26}$$

ii. Deflection:

$$\delta_{all} - \frac{2K_1 q b^4 \lambda}{E_f t_f h^2} \geq 0 \tag{27}$$

where K_1 is a coefficient based on the simply supported plate coefficient, q is the uniformly distributed load, b is the panel width, E_f is the modulus of elasticity of the facing skin, t_f is the thickness of the facing skin, h is the distance between the facing skin centres and $\delta_{al} = 0.01l$ is the allowable deflection (DNV, 2021);

iii. Facing stress:

$$\sigma_f - \frac{K_2 q b^2}{ht} \geq 0 \tag{28}$$

where K_2 is a coefficient based on the simply supported plate coefficient, $\sigma_f = \sigma_{y,al}$ is the tensile strength of aluminium 5251-T3 alloy;

iv. Core shear:

$$\tau_c - \frac{K_3 q b}{h} \geq 0 \tag{29}$$

where K_3 is a coefficient based on the simply supported plate coefficient;

v. Local compression:

$$\sigma_c - \frac{P}{A} \geq 0 \tag{30}$$

Where σ_c is the core compressive stress, P is the applied load, and A is the area of the applied load;

vi. Facing stress:

$$\sigma_f - \frac{P}{2t_f b} \geq 0 \tag{31}$$

vii. Panel buckling:

$$P_b - \frac{\pi^2 D}{l^2 + \frac{\pi^2 D}{G_c h b}} \geq 0 \tag{32}$$

where G_c is the shear modulus in the direction of applied load, and D is the bending stiffness, given by:

$$\mathrm{D} = \frac{E_f t_f h^2 b}{2} \tag{33}$$

viii. Shear crimping:

$$P_b - t_c G_c \mathrm{b} \geq 0 \tag{34}$$

ix. Skin wrinkling:

$$\sigma_{CR} - 0.5\left(G_c E_c E_f\right)^{1/3} \geq 0 \tag{35}$$

where $\sigma_{CR} = \sigma_{y,al}$ is the tensile strength of aluminium 5251-T3 alloy;

x. Intracell buckling:

$$\sigma_{CR} - 2E_f \left(\frac{t_f}{s}\right)^2 \geq 0 \tag{36}$$

where s is the cell size.

4 Results and Discussion

This chapter presents the results of the optimisation process and analyses the reliability of the obtained solutions of the Pareto-optimal front, with a brief introduction to the applied reliability model.

4.1 Pareto-optimal front

The Pareto-optimal front is obtained with the MS Excel MOO and is scaled concerning the original steel structure values by assuming a lightweight ratio, $F_1 \,/\, F_{1,0}$, with $F_{1,0} = 1{,}909.9$ t equal to the original ship's LW, and a yield stress ratio, $F_2 \,/\, F_{2,0}$, with $F_{2,0} = 310.6$ MPa, equal to the allowable stress using NV-40 steel (Figure 6).

The algorithm parameters are equal to the original ones of the MS Excel MOO, except for the maximum number of generations, which equals 200. With these parameters, the optimisation runtime is approximately 22 min. The algorithm achieved a 16.1% lightweight reduction compared to the original ship.

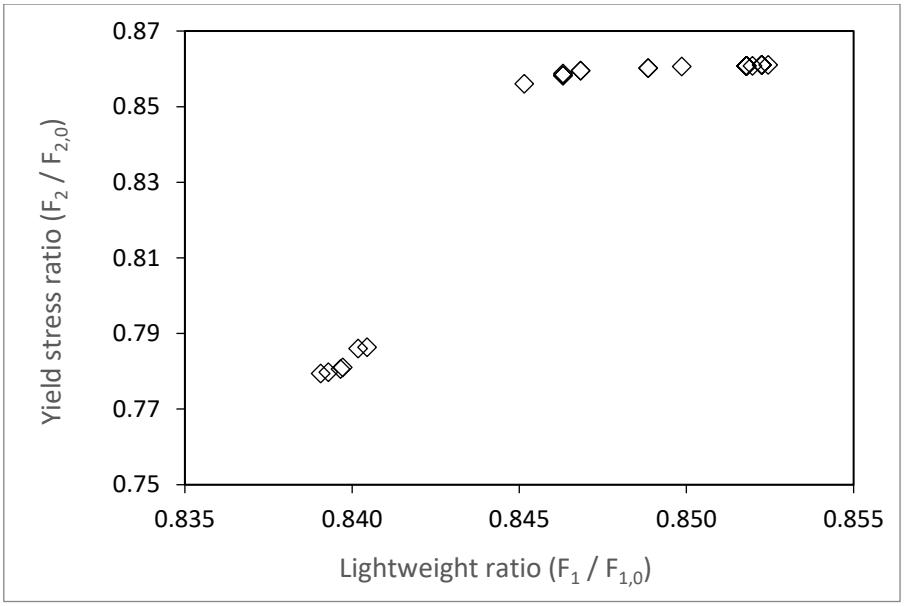

Figure 6. Pareto-optimal solutions.

4.2 Ultimate Strength and Reliability

The ultimate strength of a structure is related to the peak value of the $\varepsilon - \sigma$ curve (Figure 7), composed of an elastic region, where stress and strain are proportional to Young's modulus E, and a plastic region delimited by the yield stress σ_y. Traditionally, the real safety margin associated with allowable stress design was challenging to determine as long as the ultimate strength of the structure remained unknown. With such an approach, no detailed information on the post-buckling behaviour of members and their interactions was available; the design was usually based on elastic strength and corrected with a plasticity correction factor. The evaluation of the ultimate strength gives a better understanding of the post-buckling behaviour of the structure and, therefore, a more reliable design, where the hull girder bending capacity at any hull transverse section now must satisfy the following criterion:

$$M \leq \frac{M_U}{\gamma_R} \tag{37}$$

where γ_R is a partial safety factor for the hull girder's ultimate bending capacity as a function of prediction uncertainties and the effect of a double bottom in bending (when applicable).

The evaluation of ultimate strength was initially derived from analytical formulations. The methods used today involve the incremental-iterative method (Smith, 1977) and alternative methods, including non-linear finite element analysis, as recommended by IACS (2021).

Each solution of the true Pareto-optimal front is characterised by a specific hull girder's ultimate bending capacity; the assessment is carried out on MARS 2000 (2022), which makes use of the incremental-iterative method (Figure 9) to determine the bending moment M_i acting on the transverse section at each curvature χ_i. In this procedure, the ultimate hull girder bending moment capacity is defined as the peak value of the $\mathrm{M}-\chi$ curve (Figure 8), only considering vertical bending. The effects of shear force, torsional loading, horizontal bending moment and lateral pressure are neglected.

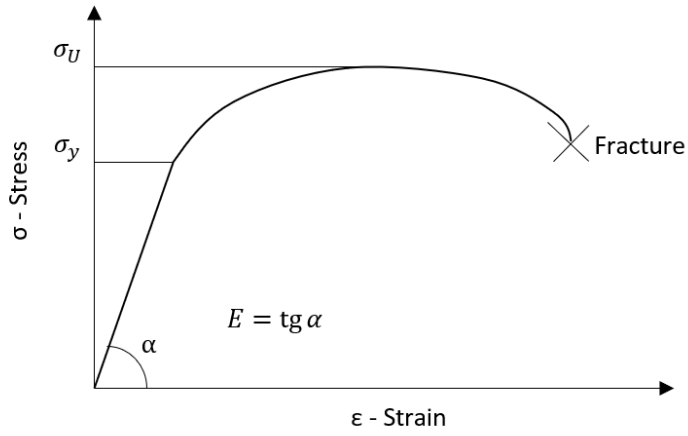

Figure 7. Stress-Strain curve of steel.

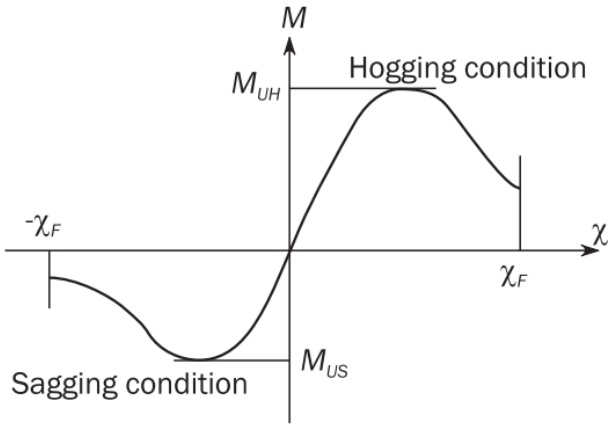

Figure 8. Bending moment capacity – curvature.

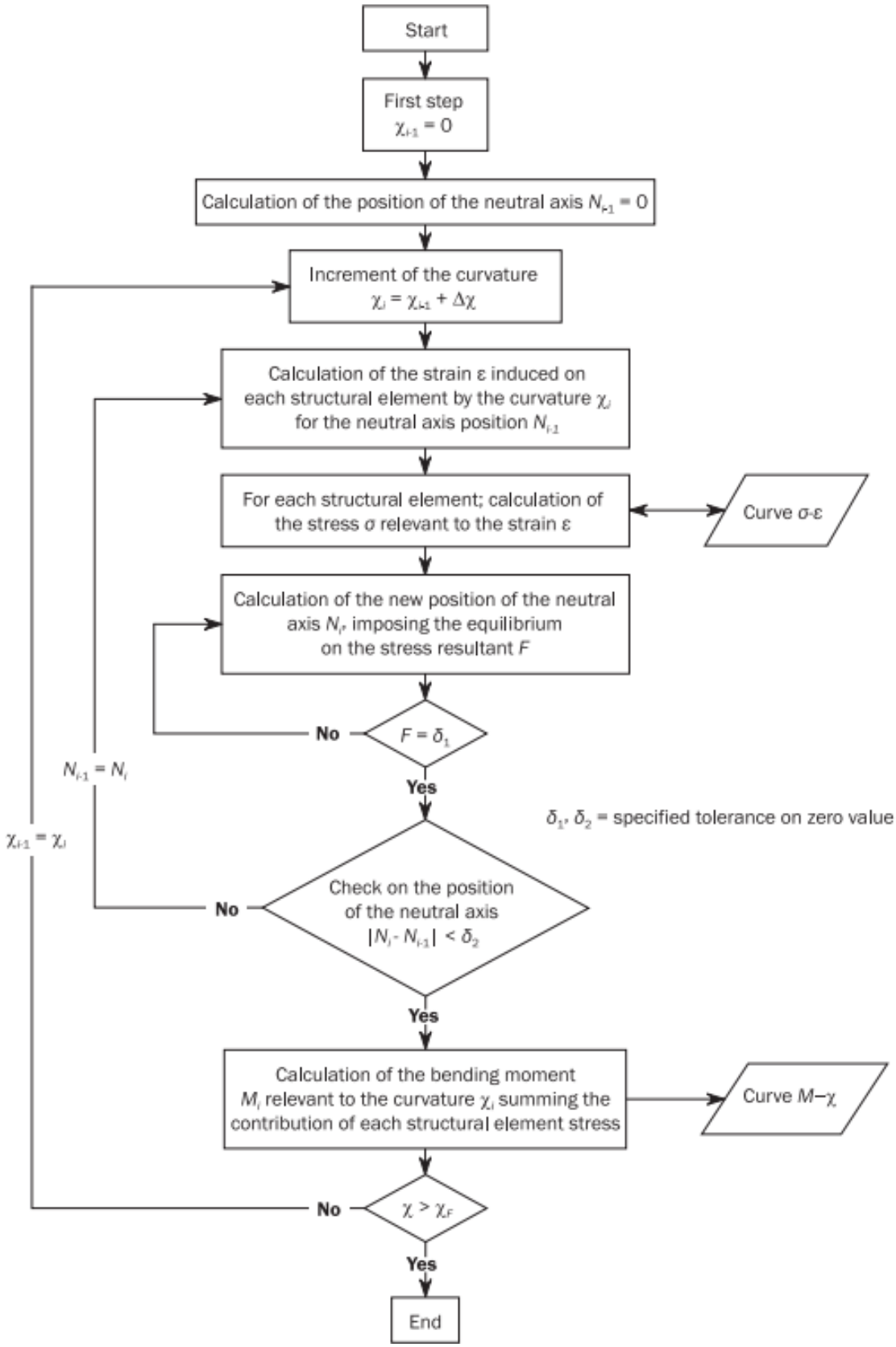

Figure 9. Flow chart of the procedure for evaluating the curve M– χ.

The evaluation of the hull girder's reliability is based on its state of operation, which can be identified as safe when it can perform its function and unsafe when it cannot. This limit is called limit-state when the structure exceeds a specific limit and cannot operate safely.

Ultimate limit-states are related to the structural collapse of part or entire structure due to corrosion, fatigue, plastic mechanism, and progressive collapse. The significant consequences of the hull girder failure require that a low probability of occurrence should characterise such a limit state.

The state of the structure can be described using resistance and load variables, $\boldsymbol{X} = (x_1, \dots, x_n)$, and therefore, the limit-state function is a function of $\mathrm{G}(x_1, \dots x_n)$ of these variables, such that the limit-state equation separating the safe from the unsafe region is given by:

$$\mathrm{G}(x_1, \dots, x_n) = \mathrm{R} - \mathrm{S} = 0 \tag{38}$$

The failure condition, based on the resistance, R, and the load effect, S, is defined as:

$$\mathrm{R} - \mathrm{S} \leq 0 \tag{39}$$

Therefore, the probability of failure can be written as follows:

$$P_f = \mathrm{P}[G(x_1, \dots, x_n) \leq 0] \tag{40}$$

In general, there is not enough information on the distribution of the limit-state variables. Therefore, these are replaced with statistical distributions, such as Normal, Lognormal, Weibull and Gumbel distributions.

The FORM method introduced by Hasofer and Lind (Hasofer & Lind, 1974) allows for quantifying the reliability of the structure with a β-reliability index. This index can be defined as the largest β satisfying the requirement "The distance from the origin to the failure region $G^*(\mathrm{R}, \mathrm{S})$ must be greater than β," as illustrated in Figure 10.

In other words, the β-reliability index is the shortest distance from the origin to the transformed limit-state function into a standard normal space. This transformation can be achieved as follows:

$$U_1 = \frac{R - E(R)}{\sigma_R}, \quad \mathrm{R} = U_1 \sigma_R + \mathrm{E}(\mathrm{R}) \tag{41}$$

$$U_2 = \frac{S - E(S)}{\sigma_S}, \quad \mathrm{S} = U_2 \sigma_S + \mathrm{E}(\mathrm{S}) \tag{42}$$

where σ_i is the standard deviation, and $\mathrm{E}(i)$ is the mean value. Finally, the β-reliability index is the solution to the constrained optimisation problem in the standard normal space:

$$\begin{aligned} &Minimise: && \beta(U) = \sqrt{U^T U} \\ &Subject\ to: && g(U) = 0 \end{aligned} \tag{43}$$

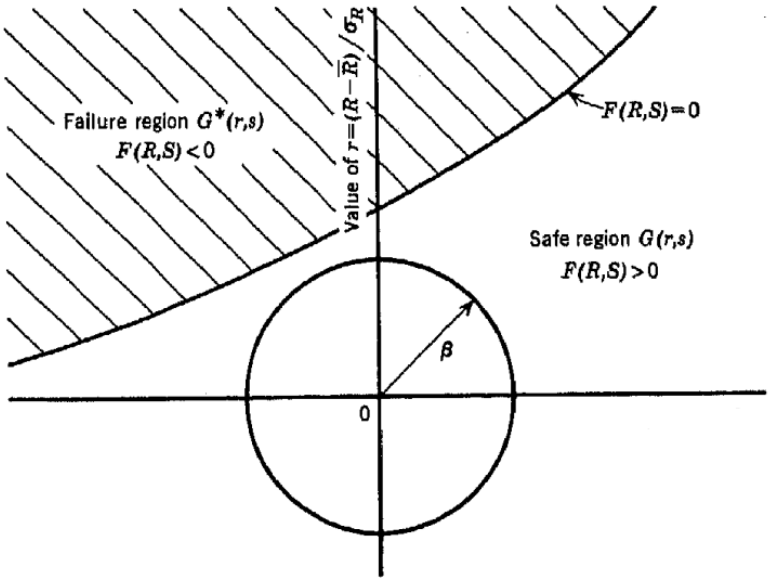

Figure 10. Reliability index for two variables (Hasofer & Lind, 1974).

The limit-state function of the reliability assessment is based on the ship hull's ultimate strength, the vertical still water bending moment and the wave-induced bending moments, defined as:

$$\mathrm{G} = \tilde{x}_U \cdot \widetilde{M}_U - \tilde{x}_{SW} \cdot \widetilde{M}_{SW} - \tilde{x}_W \tilde{x}_S \cdot \widetilde{M}_{WV} \tag{44}$$

where M_U is the ultimate bending moment, M_{SW} is the still water bending moment, M_{WV} is the wave-induced bending moment, x_U is the model uncertainty on ultimate strength, x_{SW} is the uncertainty in the model of predicting the still water bending moment, x_W takes into account nonlinearities in sagging and x_S is the wave bending moment error due to linear see-keeping analysis. The variables representing the model uncertainty were introduced in (Parunov, et al., 2015) in their work on the structural reliability assessment of a container ship at the time of the accident (Table 8).

Table 8. Uncertainty factors in the limit-state function.

Parameter	Distribution	Mean	Standard deviation
x_U	Lognormal	1.10	0.11
x_{SW}	Normal	1.00	0.05
x_W	Normal	1.00	0.10
x_S	Normal	0.89	0.15

The ultimate bending moment is fitted to the Lognormal probability density function:

$$f_{M_U} = \frac{1}{M_U \sigma_{M_U \sqrt{2\pi}}} \cdot e^{-\frac{\ln\left(M_U - \mu_{M_U}\right)}{2\sigma^2_{M_U}}} \tag{45}$$

$$\sigma_{M_U} = \sqrt{\ln(COV^2 + 1)} \tag{46}$$

$$\mu_{M_U} \rightarrow F^{-1}_{M_U}\left(0.05,\, \mu_{M_U}, \sigma_{M_U}\right) = M_U^{5\%} \tag{47}$$

where $M_U^{5\%}$ is the 5% confidence level ultimate bending moment calculated by MARS 2000, μ_{M_U} is the mean calculated iteratively for each M_U to return $M_U^{5\%}$, $\sigma_{M_U}^2$ is the variance, and COV is the coefficient of variation assumed to equal 0.08.

The still water bending moment is fitted to the Normal distribution. Regression equations define the mean value and standard deviation of the still water bending moment as a function of the length of the ship, L, and the deadweight ratio, $W = DWT/Full\ Load$, as proposed in Guedes Soares and Moan (1988), Guedes Soares (1990):

$$\bar{M}_{SW,max} = 114.7 - 105.6W - 0.154L \tag{48}$$

$$\sigma\left(M_{SW,max}\right) = 17.4 - 7W + 0.035L \tag{49}$$

$$\bar{M}_{SW} = \frac{\bar{M}_{SW,max} \cdot M_{SW,CS}}{100} \tag{50}$$

$$\sigma(M_{SW}) = \frac{\sigma\left(M_{SW,max}\right) \cdot M_{SW,CS}}{100} \tag{51}$$

where $\bar{M}_{SW} = 3.1\ MNm$ is the mean still water bending moment, $\sigma\left(M_{SW,max}\right) = 24.3\ MNm$ is the still water bending moment standard deviation, W is assumed to equal 0.9 for full load conditions, $M_{SW,CS} = -159.9\ MNm$ is the still water bending moment according to DNV (2021).

The wave-induced bending moment for strength assessment, given by the Classification Societies Rules at a probability level of 10^{-8}, may be modelled as a Weibull distribution considering that the wave-induced bending moment can be represented as a stationary Gaussian process:

$$F_{M_{VW}} = 1 - \exp\left(\frac{M_{VW}}{q}\right)^h \tag{52}$$

where q is the Weibull scale parameter, and h is the shape parameter, accordingly to (DNV, 2010):

$$q = \frac{M_{W,CS}}{\ln(10^8)^{1/h}} \tag{53}$$

$$h = 2.26 - 0.54\log_{10}(L) \tag{54}$$

The distribution of the extreme values of the wave-induced bending moment at a random point over a specified time may be modelled as a Gumbel distribution (Guedes Soares, et al., 1996). The Gumbel distribution is derived from the Weibull factors as a function of the location parameter, α_m, and the scale parameter, β_m:

$$F_{M_W} = \exp\left\{-\exp\left(-\frac{M_{W,e} - \alpha_m}{\beta_m}\right)\right\} \tag{55}$$

$$\alpha_m = q(\ln(n))^h \tag{56}$$

$$\beta_m = \frac{q}{h}(\ln(n))^{(1-h)/h} \quad (57)$$

The number of cycles, n, is based on a reference time period, T_r, equal to one year for an average wave period T_W of 8s:

$$n = \frac{p \cdot T_r \cdot 365 \cdot 24 \cdot 3600}{T_W} \quad (58)$$

where $M_{W,e} = \sqrt{2\sigma_{MW}^2 \ln n}$ is a random variable that represents the extreme values of the vertical wave-induced bending moment of the reference time T_r, and p is the partial time in full load seagoing conditions, equal to 0.4.

The β-reliability indexes of the Pareto-optimal solutions (Table 9) are computed with VBA and compared with a target β-reliability index between 3.09 and 3.71 (DNV, 1992).

Table 9. β-reliability indexes of the Pareto-optimal solutions.

Sol. Num.	Lightweight ratio	Yield stress ratio	M_U [MNm]	α_m	β_m	β
1	0.839	0.779	810.1	926.8	74.1	4.43
2	0.839	0.780	808.7	925.1	74.0	4.42
5	0.840	0.781	803.1	918.8	73.5	4.39
7	0.840	0.781	802.7	918.3	73.5	4.38
10	0.840	0.786	785.1	898.2	71.9	4.27
11	0.840	0.786	785.1	898.2	71.9	4.27
12	0.845	0.856	724.8	829.2	66.3	3.87
17	0.846	0.858	695.9	796.1	63.7	3.67
18	0.846	0.859	694.0	794.0	63.5	3.66
19	0.847	0.859	700.5	801.4	64.1	3.70
21	0.849	0.860	690.3	789.8	63.2	3.63
22	0.850	0.861	687.8	786.9	62.9	3.61
24	0.852	0.861	681.3	779.4	62.4	3.57
28	0.852	0.861	681.1	779.2	62.3	3.57
29	0.852	0.861	687.6	786.6	62.9	3.61
31	0.852	0.861	687.6	786.7	62.9	3.61
33	0.852	0.861	687.3	786.2	62.9	3.61

The results show that the design optimisation tends to assume the properties of a single-objective optimisation, as higher ultimate bending capacities characterise the lighter design solutions and, therefore, higher β-indexes of reliability (Figure 11-Figure 12).

This can be justified by changing the midship sectional properties of the Pareto-optimal solutions. The selection of higher tensile strength steel at the bottom, and lower tensile strength at the deck, towards higher β-reliability indexes (Figure 13), has an impact on the scantling requirements of the structural members. This selection contributes to a shift of the neutral axis towards the deck, positively impacting the buckling of structural members and, therefore, higher values of the ultimate bending capacity of the hull girder. The ultimate bending moment does not account for non-continuous structures, including hatch coaming and bilge keel. The contribution of these structures to the ultimate bending capacity needs to be evaluated by FEM analysis.

The obtained β-reliability indexes account for an equivalent thickness of the sandwich panels of 22mm on average. The model representing sandwich panels as equivalent steel plates tends to overestimate the

ultimate bending capacity. The midship section is made of two different materials, but artificially this is translated into a single homogeneous material, where no interaction between two panels of different materials is considered. AHS represent an excellent application for local pressure loads, as their core is parallel to the load. In the case of axial loads, the core does not contribute to the panel's strength. Therefore, the equivalent thickness approach does not represent the most suitable methodology for this problem. More analysis is needed for the honeycomb core subjected to axial pressure concerning the buckling failure. Furthermore, the redistribution of the axial loads between steel panel plates and AHS may not be smooth as considered. This aspect needs to be resolved in future studies.

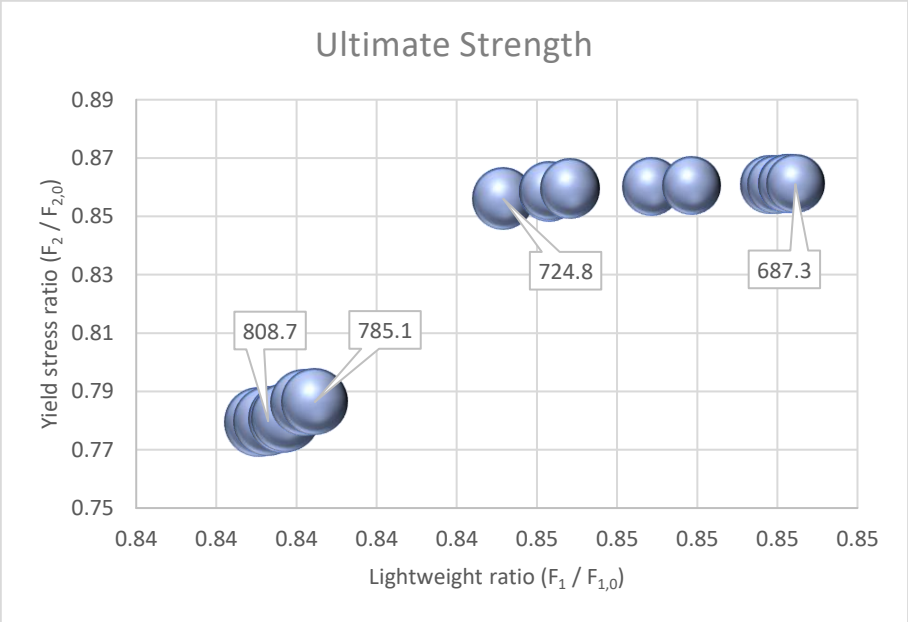

Figure 11. Ultimate bending capacity in MNm of the Pareto-optimal solutions.

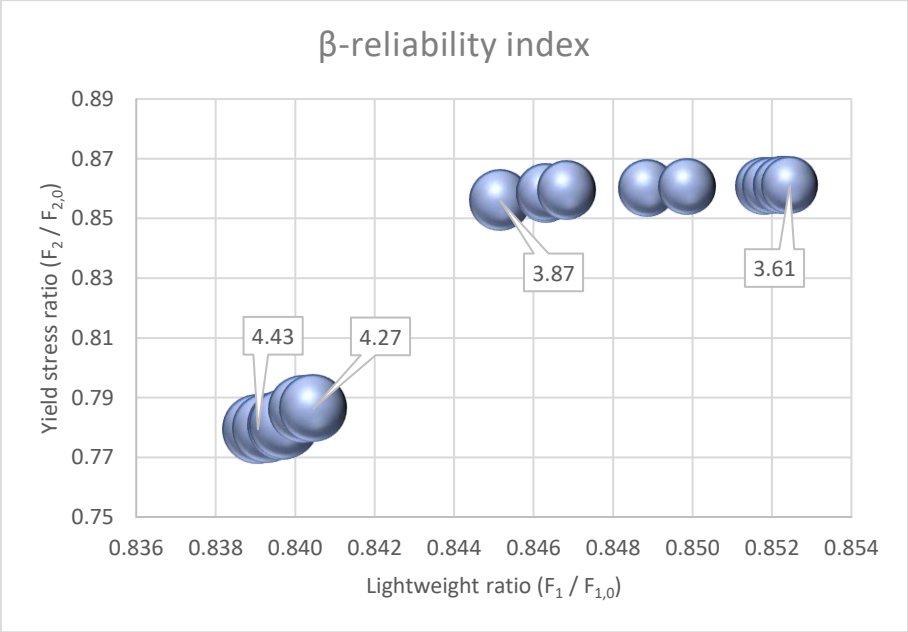

Figure 12. β-reliability indexes compared to target range of 3.09 - 3.71.

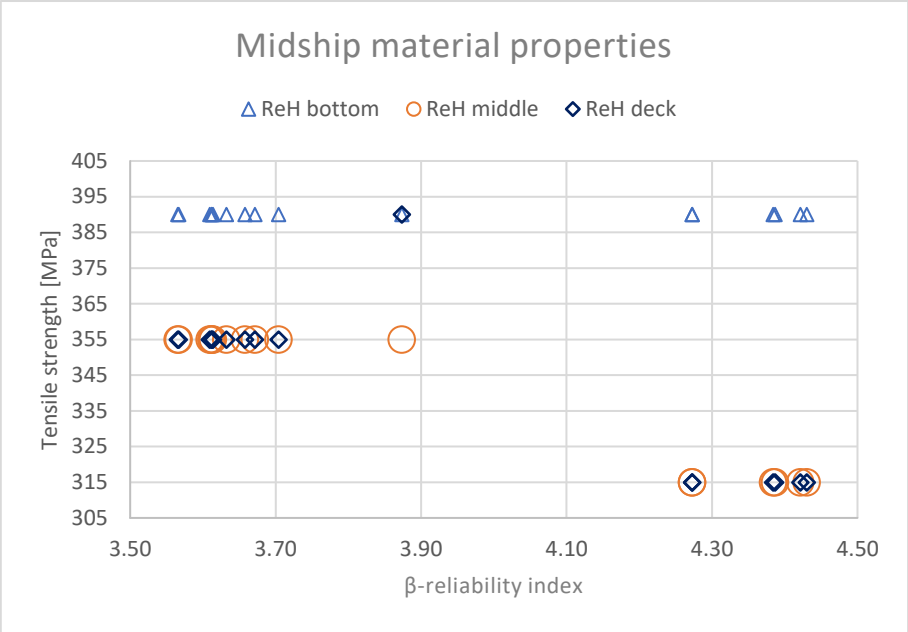

Figure 13. Steel tensile strength of the Pareto-optimal solutions.

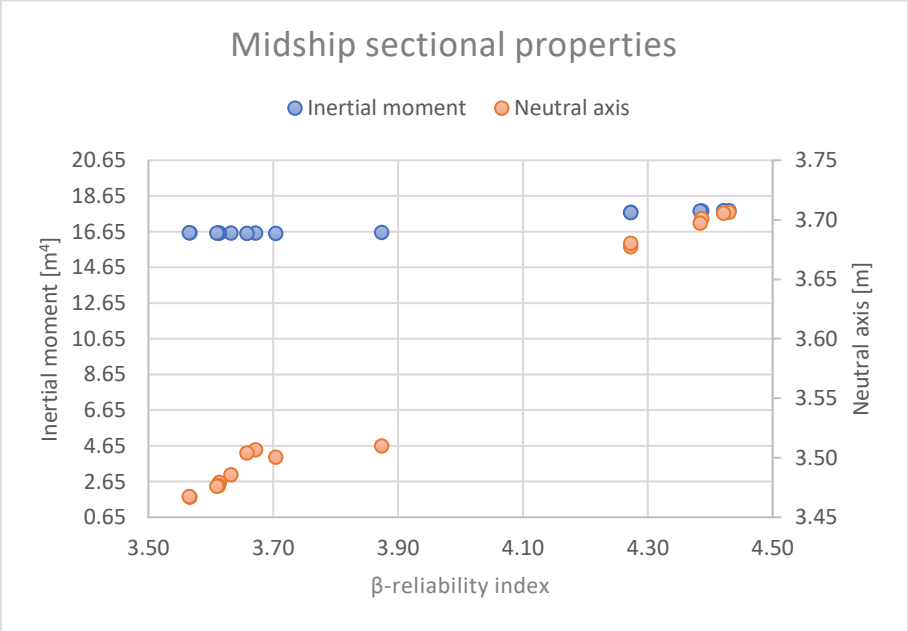

Figure 14. Inertial moment and position of the neutral axis of the Pareto-optimal solutions.

The capital cost assessment is based on the cost of steel and AHS. The cost of a sandwich panel of varying thicknesses of 3.2m x 1.5m is 520 EUR (Made in China, 2022). The average weight of a sandwich panel is 200kg, leading to a price of about 2600 EUR/t. Together with the steel prices shown in Table 10, Eq. (11) may be adapted as follows:

$$C_{Ship} = 0.034L^{1.7}B^{0.7}D^{0.4}C_B^{0.5}(0.2 \cdot \bar{C}_{steel} + 0.8(\%W_{AHS} \cdot C_{AHS} + (1 - \%W_{AHS}) \cdot \bar{C}_{steel})) \quad (59)$$

It is assumed that the cargo space represents 80% of the ship's length, where the AHS is employed. The cost of this portion takes into consideration the percentage of AHS weight in the midship section, $\%W_{AHS}$, to calculate the cost of the ship, with the respective price of AHS. On average, this amounts to 7.2% of the midship section's weight (Table 11).

The remaining part, composed of steel, considers an average cost among the steel prices in Table 10. The original ship cost is 1,580,452€.

Table 10. Detail of Steel and AHS prices (Made in China, 2022).

Item	Cost	Unit
235 MPa Steel	750	EUR/t
315 MPa Steel	780	EUR/t
355 MPa Steel	890	EUR/t
390 MPa Steel	890	EUR/t
AHS	2600	EUR/t

Table 11. Economic assessment of the Pareto-optimal solutions.

Sol. Num.	Lightweight ratio	Yield stress ratio	β	LW	$\%W_{AHS}$	C_{Ship}	Cost increase
1	0.839	0.779	4.43	-16.1%	6.8%	1,765,726 €	11.7%
2	0.839	0.780	4.42	-16.1%	6.8%	1,765,569 €	11.7%
5	0.840	0.781	4.39	-16.0%	6.8%	1,765,486 €	11.7%
7	0.840	0.781	4.38	-16.0%	6.8%	1,765,358 €	11.7%
10	0.840	0.786	4.27	-16.0%	6.9%	1,767,977 €	11.9%
11	0.840	0.786	4.27	-16.0%	6.9%	1,767,827 €	11.9%
12	0.845	0.856	3.87	-15.5%	7.4%	1,781,773 €	12.7%
17	0.846	0.858	3.67	-15.4%	7.4%	1,781,335 €	12.7%
18	0.846	0.859	3.66	-15.4%	7.4%	1,781,343 €	12.7%
19	0.847	0.859	3.70	-15.3%	7.4%	1,781,105 €	12.7%
21	0.849	0.860	3.63	-15.1%	7.5%	1,782,312 €	12.8%
22	0.850	0.861	3.61	-15.0%	7.4%	1,781,933 €	12.7%
24	0.852	0.861	3.57	-14.8%	7.3%	1,778,668 €	12.5%
28	0.852	0.861	3.57	-14.8%	7.3%	1,778,587 €	12.5%
29	0.852	0.861	3.61	-14.8%	7.4%	1,781,252 €	12.7%
31	0.852	0.861	3.61	-14.8%	7.4%	1,781,252 €	12.7%
33	0.852	0.861	3.61	-14.8%	7.4%	1,781,194 €	12.7%

A comparison between the two solutions and the original ship is shown in the following figures. The midship section was divided into three areas concerning steel tensile strength (Figure 15); the bottom part of the structure has a constant composition of 390 MPa steel, whereas the remaining part tends to 315 MPa for higher β-reliability indexes. The hull girder strength does not significantly differ between the original ship and the two solutions (Figure 16). The local strength related to the strakes shows some critical areas in the bottom (Figure 17), similar to the original, despite local reinforcement with flat bars. This is related to minimum thickness requirements, which result in different software. The reason for this non-correspondence may be related to using two different Class societies, DNV and BV. The local strength related to the stiffeners also shows some critical areas in the bottom related to minimum thicknesses. The constraints on buckling in the model use the gross thickness, whereas the rules use a net thickness approach applied to the bulb profiles. The determination of the net area post-corrosion may represent a complicated calculation because of the geometry of the bulb profiles. To overcome this problem, an increase of 10% of the bulb flat area requirement may be applied, leading to the selection of a more extensive profile. However, this procedure may lead to the over-dimensioning of the bulb flats. Therefore, a careful check should be done.

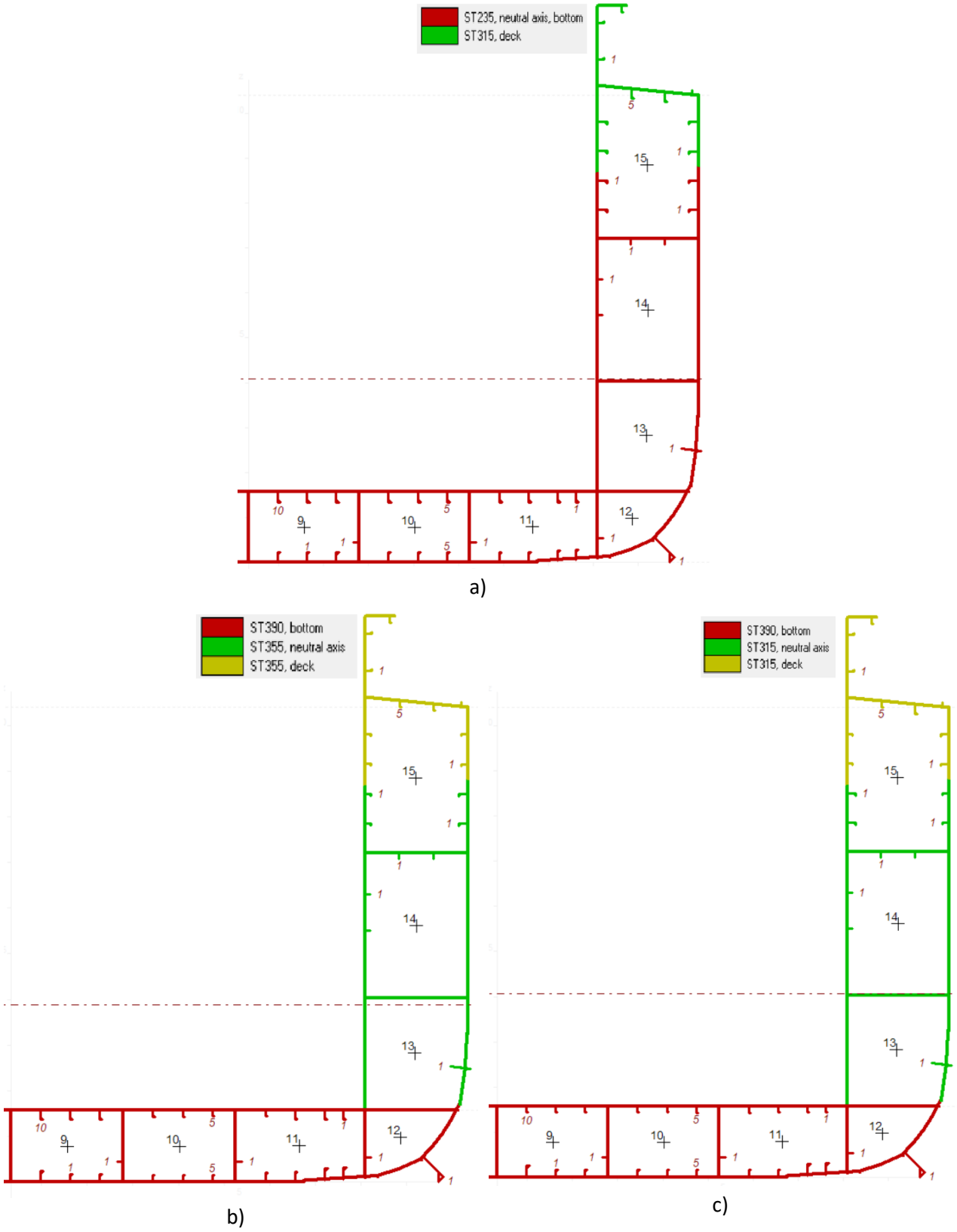

Figure 15. Midship section material properties: a) Original ship b) β=3.61 c) β=4.43.

a)

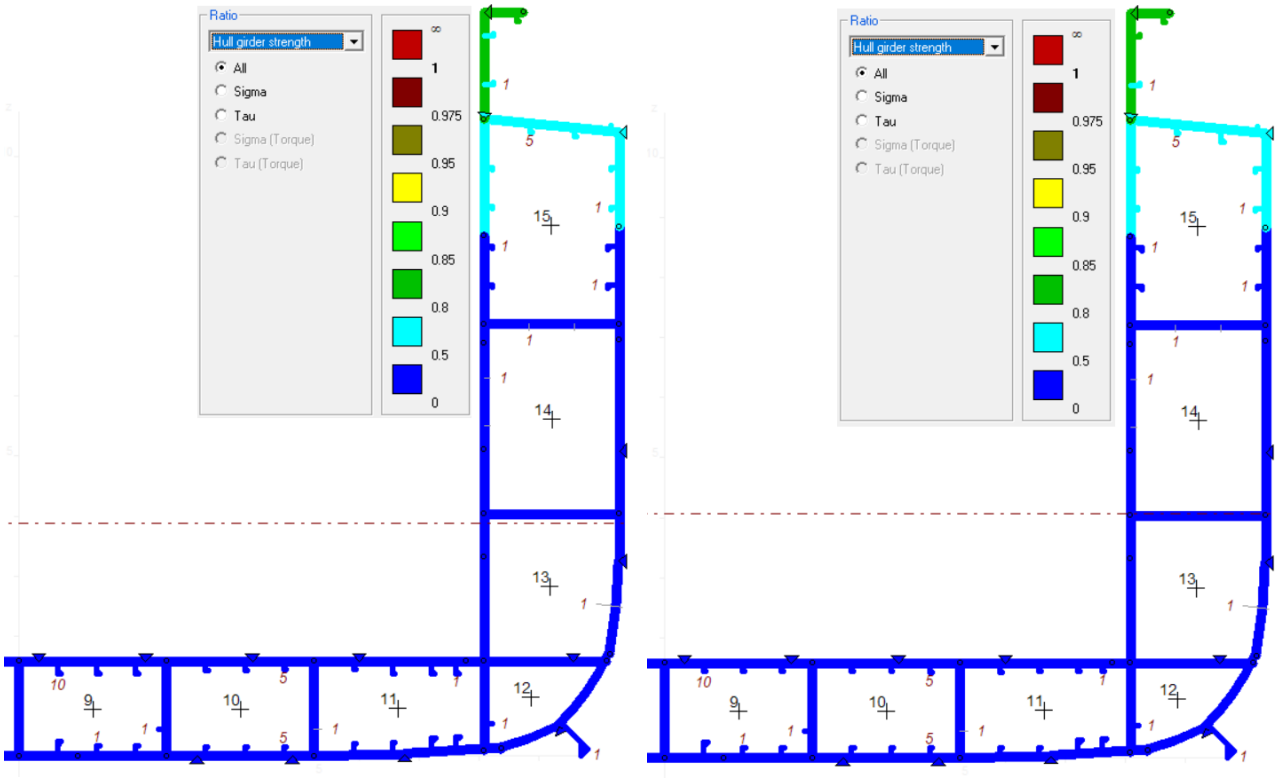

b) c)

Figure 16. Hull girder strength: a) Original ship b) β=3.61 c) β=4.43.

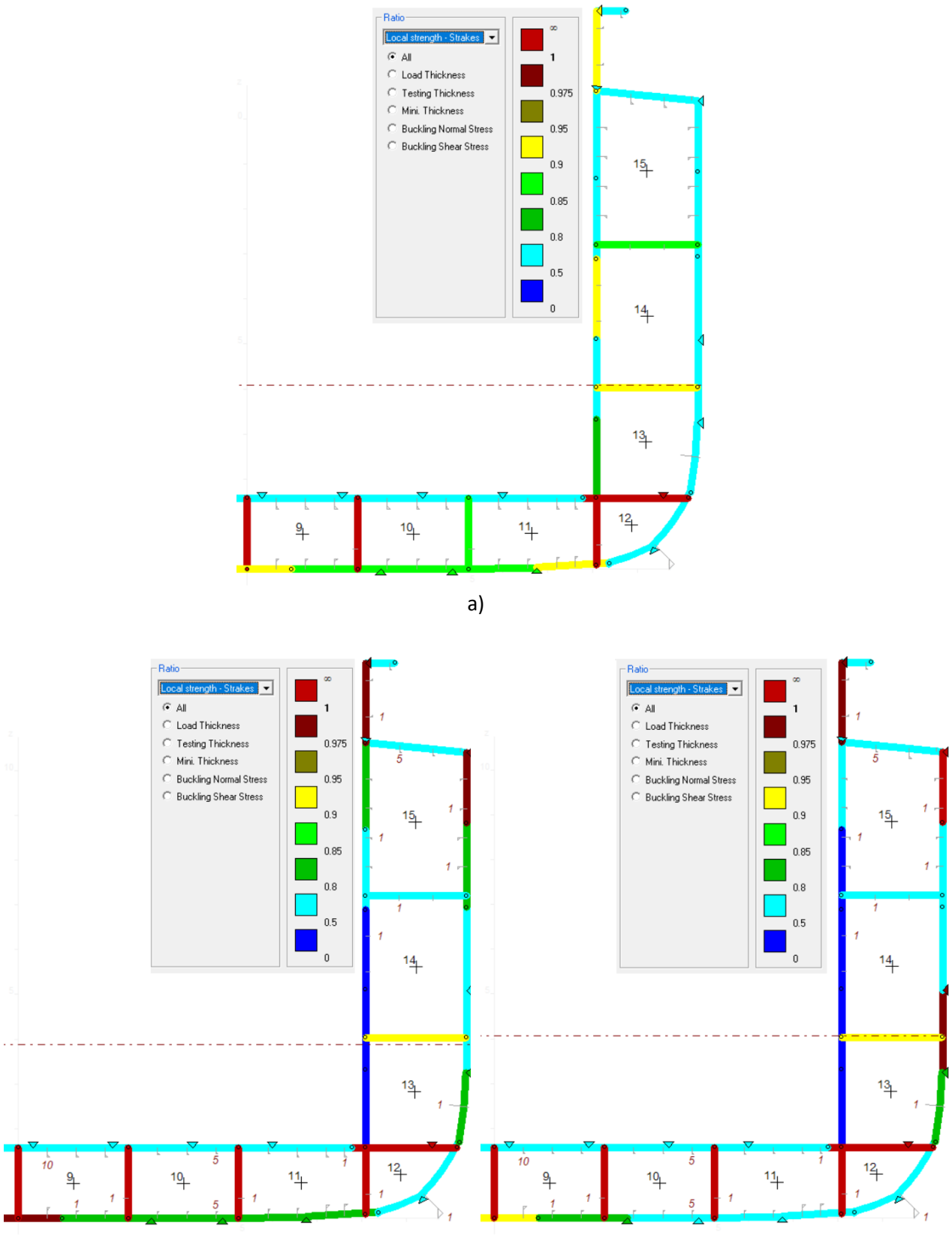

Figure 17. Local strength - Strakes: a) Original ship b) β=3.61 c) β=4.43.

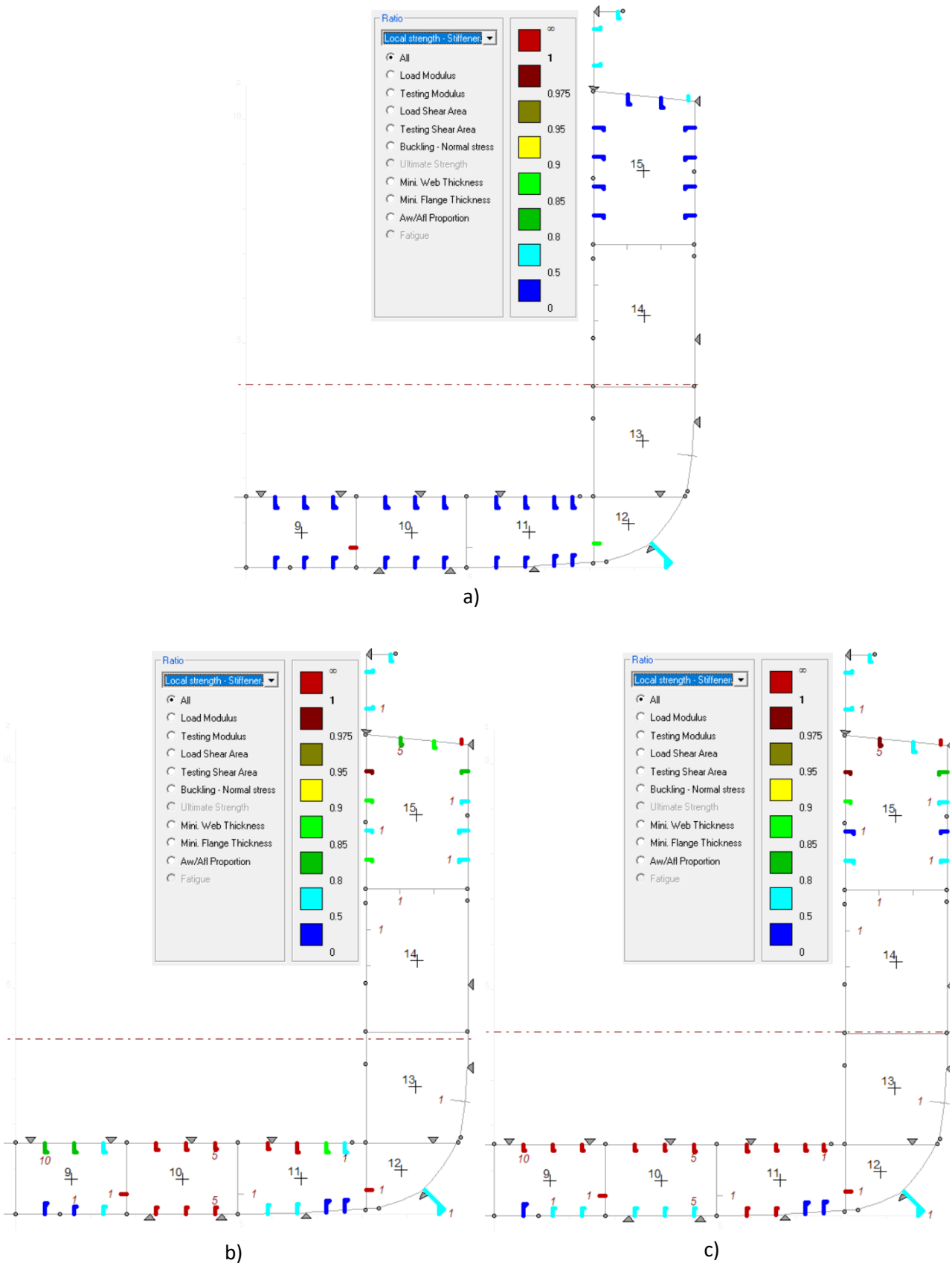

Figure 18. Local strength - Stiffeners: a) Original ship b) β=3.61 c) β=4.43.

5 Conclusion

A risk-based hybrid ship hull structural design and optimisation was presented. The hybrid structure comprises honeycomb sandwich panels of aluminium 5251-T3 alloy replacing the vertical inner cargo shell. The optimisation is based on discrete variables employing a genetic algorithm, with ship lightweight and stress at the deck as objective functions. The optimisation aims to develop an automatic algorithm on VBA capable of joining the ship model, the EMOO software, the ultimate strength calculation with MARS 2000 and a β-reliability index code. The weight savings range between 14.8% - 16.1% concerning the original ship. High tensile steel of 390 MPa at the bottom and 315 MPa steel at the mid-section and deck contribute to lighter and more reliable solutions. The obtained β-reliability indexes range between 3.61 and 4.43; the values are deemed overestimated due to the equivalent thickness approach applied in the modelling of the AHS. A deeper understanding of the interaction between steel panel plates and AHS is required better to estimate the hull girder's ultimate bending capacity. The connection between these two structures creates some problems due to the assumed redistribution of the axial loads to be smooth, which in reality, may be different. The honeycomb core is an excellent application for local pressure; however, more analysis is needed for the honeycomb core subjected to axial pressure concerning buckling failure. The material cost increase for the lightweight hybrid structure is about 12.4% considering an AHS cost of 2,600 EUR/ton. The economic advantage of a hybrid structure requires additional investment analysis based on a ship's typical voyage and the expected duration of the investment.

Further studies in this direction could include ultimate bending capacity as an objective function by developing an incremental-iterative method code to be included as part of the VBA algorithm. Such code would require less than one hour to obtain a fully optimised structure. In the case of standard midship sections, the already developed algorithm is expected to obtain reliable solutions without overestimating the β-reliability indexes. Furthermore, the work presented could be implemented as software, including a user interface with drawing tools and a database of rules applicable to optimise different types of ships in a preliminary design stage.

6 Annex

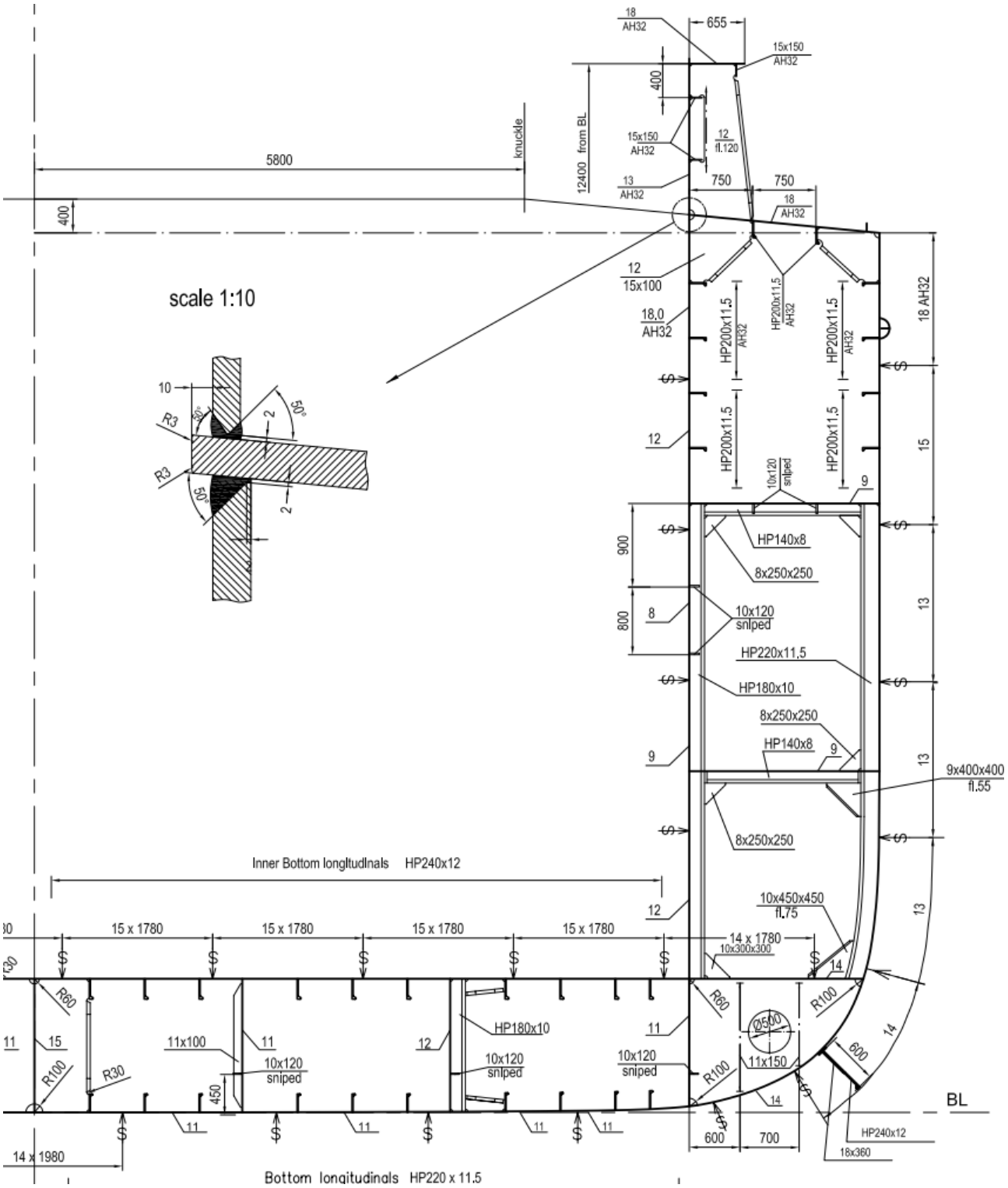

Figure 19. Drawing of the original midship section.

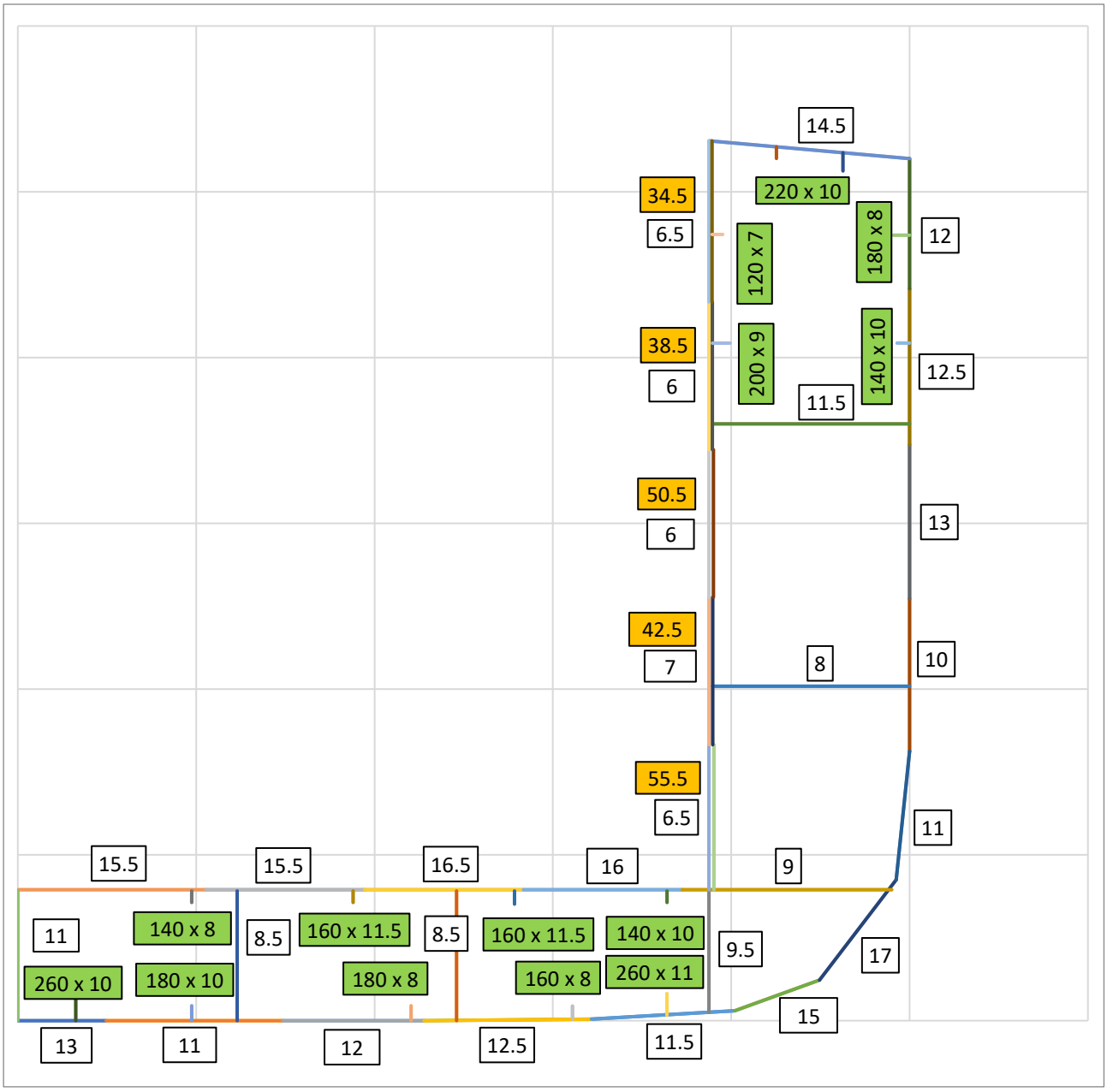

Figure 20. Drawing of the midship section for β = 4.43.

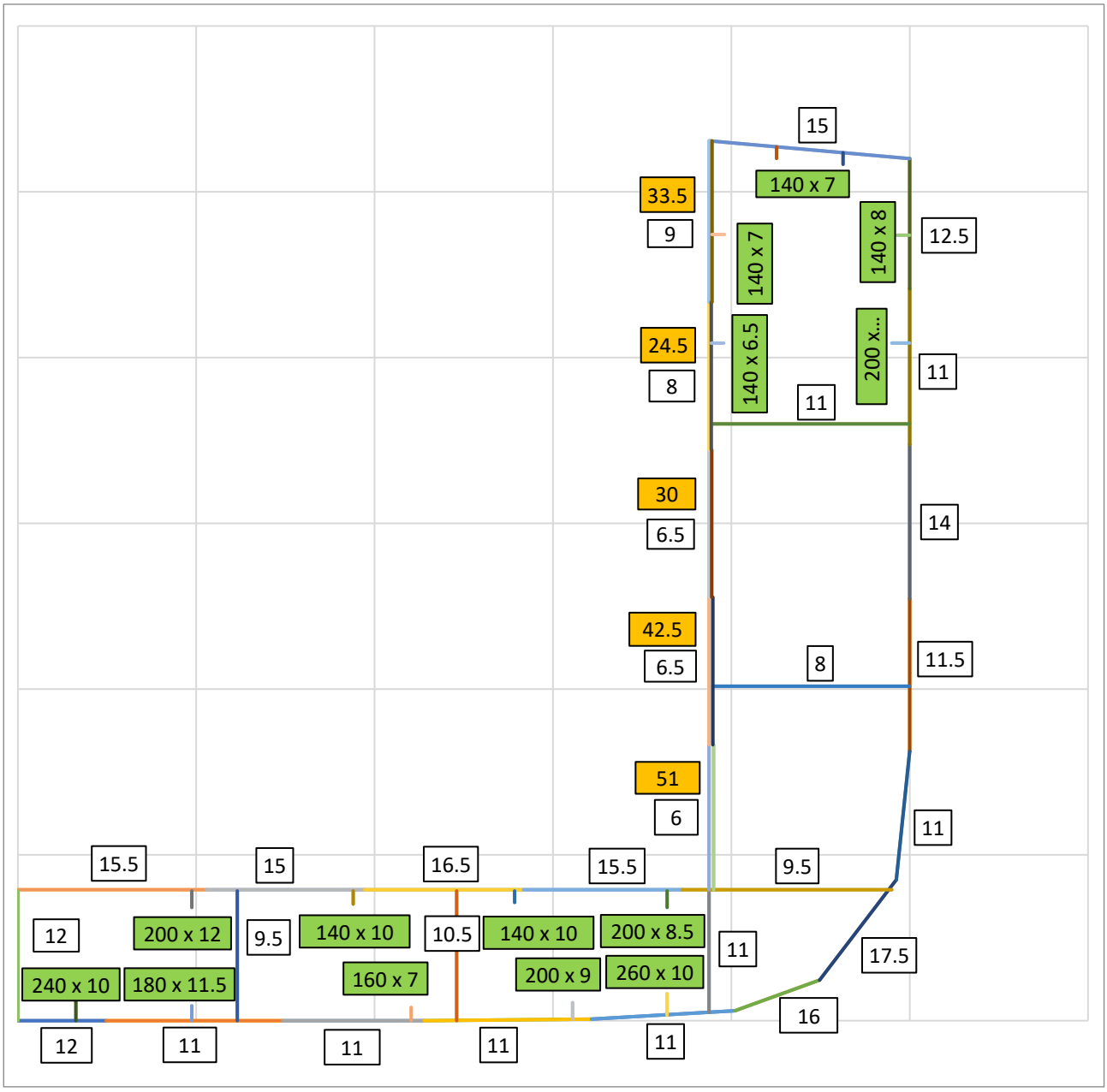

Figure 21. Drawing of the midship section for β = 3.61.

Dimensions and properties

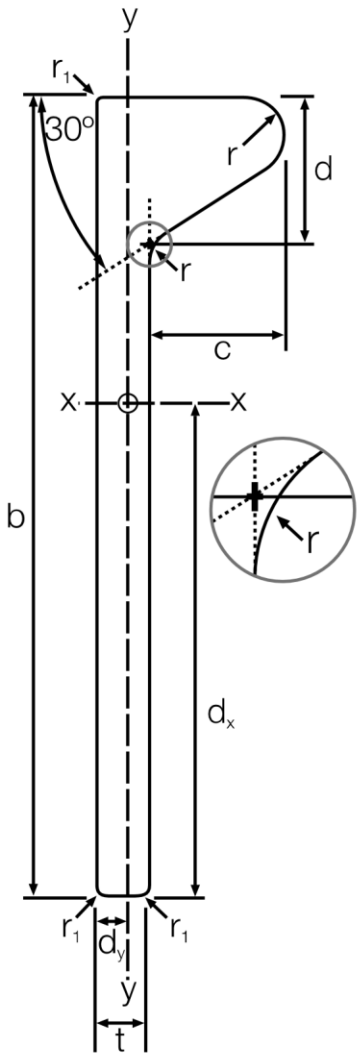

Width b [mm]	Thickness t [mm]	Mass per Unit Length G [kg/m]	Bulb Height c [mm]	Bulb Width d [mm]	Bulb Radius r [mm]	Area of cross-section F [cm²]	Surface Area U [m²/m]
120	6	7.31	17	17.7	5	9.31	0.276
	7	8.25	17	17.7	5	10.5	0.278
	8	9.19	17	17.7	5	11.7	0.280
140	6.5	9.21	19	19.7	5.5	11.7	0.319
	7	9.74	19	19.7	5.5	12.4	0.320
	8	10.8	19	19.7	5.5	13.8	0.322
	10	13.0	19	19.7	5.5	16.6	0.326
160	7	11.4	22	22.2	6	14.6	0.365
	8	12.7	22	22.2	6	16.2	0.367
	9	14.0	22	22.2	6	17.8	0.369
	11.5	17.3	22	22.2	6	21.8	0.374
180	8	14.8	25	25.5	7	18.9	0.411
	9	16.2	25	25.5	7	20.7	0.413
	10	17.6	25	25.5	7	22.5	0.415
	11.5	19.7	25	25.5	7	25.2	0.418
200	8.5	17.8	28	28.8	8	22.6	0.456
	9	18.5	28	28.8	8	23.6	0.457
	10	20.1	28	28.8	8	25.6	0.459
	11	21.7	28	28.8	8	27.6	0.461
	12	23.2	28	28.8	8	29.6	0.463
220	9	21.0	31	32.1	9	26.8	0.501
	10	22.8	31	32.1	9	29.0	0.503
	11	24.5	31	32.1	9	31.2	0.505
	12	26.2	31	32.1	9	33.4	0.507
240	9.5	24.4	34	35.4	10	31.2	0.546
	10	25.4	34	35.4	10	32.4	0.547
	11	27.4	34	35.4	10	34.9	0.549
	12	29.3	34	35.4	10	37.3	0.551
260	10	28.3	37	38.7	11	36.1	0.593
	11	30.3	37	38.7	11	38.7	0.593
	12	32.4	37	38.7	11	41.3	0.595
280	10.5	32.4	40	42.0	12	41.2	0.636
	11	33.5	40	42.0	12	42.6	0.637
	12	35.7	40	42.0	12	45.5	0.639
	13	37.9	40	42.0	12	48.4	0.641
300	11	36.7	43	45.3	13	46.7	0.681
	12	39.0	43	45.3	13	49.7	0.683
	13	41.5	43	45.3	13	52.8	0.685
320	11.5	41.2	46	48.6	14	52.6	0.727
	12	42.5	46	48.6	14	54.2	0.728
	13	45.0	46	48.6	14	57.4	0.730
	14	47.5	46	48.6	14	60.6	0.732
340	12	46.1	49	52.0	15	58.8	0.772
	13	48.8	49	52.0	15	62.2	0.774
	14	51.5	49	52.0	15	65.5	0.776
	15	54.2	49	52.0	15	69.0	0.778
370	12.5	53.1	53.5	56.9	16.5	67.8	0.839
	13	54.6	53.5	56.9	16.5	69.6	0.840
	14	57.5	53.5	56.9	16.5	73.3	0.842
	15	60.5	53.5	56.9	16.5	77.0	0.844
	16	63.5	53.5	56.9	16.5	80.7	0.846
400	13	60.8	58	61.9	18	77.4	0.907
	14	63.9	58	61.9	18	81.4	0.908
	15	67.0	58	61.9	18	85.4	0.910
	16	70.2	58	61.9	18	89.4	0.912
430	14	70.6	62.5	66.8	19.5	89.7	0.975
	15	73.9	62.5	66.8	19.5	94.1	0.976
	17	80.6	62.5	66.8	19.5	103.0	0.980
	20	90.8	62.5	66.8	19.5	115.0	0.986

Additional sizes may be available by agreement: 80 & 100 DIN range
180, 200, 230 and 250 JIS range

* Values for H are taken about the line of attachment.

Distance of Centre of Gravity		Second Moment of Area		Elastic Modulus		Radius of Gyration		Warping Constant	Torsional Constant
d_x [mm]	d_y [mm]	Axis x - x cm^4	Axis y - y cm^4	Axis x - x cm^3	Axis y - y cm^3	Axis x - x cm	Axis y - y cm	H* $[cm^6(x10^3)]$	J $[cm^4]$
72.0	5.3	133	2.34	18.4	4.42	3.78	0.50	0.242	1.595
70.7	5.6	148	2.70	21.0	4.82	3.75	0.51	0.251	2.100
69.6	6.0	164	3.10	23.6	5.17	3.74	0.51	0.263	2.773
83.7	5.8	228	3.57	27.3	6.16	4.41	0.55	0.504	2.383
83.1	5.9	241	3.80	29.0	6.44	4.41	0.55	0.508	2.708
81.8	6.3	266	4.32	32.5	6.86	4.39	0.56	0.528	3.501
79.2	7.0	316	5.56	39.9	7.94	4.36	0.58	0.575	5.752
96.6	6.4	373	5.86	38.6	9.16	5.05	0.63	1.12	3.681
94.9	6.8	411	6.55	43.3	9.63	5.04	0.64	1.16	4.600
93.6	7.1	448	7.32	47.9	10.3	5.02	0.64	1.20	5.763
91.1	8.1	544	9.62	59.8	11.9	5.00	0.66	1.31	9.936
109	7.4	609	9.90	55.9	13.4	5.68	0.72	2.45	6.352
107	7.7	665	10.93	62.1	14.2	5.67	0.73	2.51	7.686
106	8.1	717	12.05	67.8	14.9	5.65	0.73	2.58	9.328
104	8.6	799	13.93	76.8	16.2	5.63	0.74	2.71	12.44
122	8.2	902	15.07	74.0	18.4	6.32	0.82	4.67	9.129
121	8.4	941	15.76	77.7	18.8	6.31	0.82	4.72	9.924
119	8.7	1020	17.21	85.0	19.8	6.31	0.82	4.83	11.70
118	9.0	1090	18.77	92.3	20.9	6.28	0.82	4.93	14.00
117	9.4	1160	20.46	99.6	21.8	6.26	0.83	5.09	16.65
136	9.1	1296	22.03	95.3	24.2	6.95	0.91	8.64	13.24
134	9.3	1400	23.89	105	25.7	6.95	0.91	8.80	15.31
132	9.6	1500	25.86	113	26.9	6.93	0.91	8.98	17.81
130	10.0	1590	27.98	122	28.0	6.90	0.92	9.18	20.76
148	9.9	1800	31.15	123	31.5	7.60	1.00	14.8	18.16
147	10.0	1860	32.34	126	32.3	7.58	1.00	14.9	19.37
146	10.3	2000	34.81	137	33.8	7.57	1.00	15.3	22.46
144	10.6	2130	37.43	148	35.3	7.56	1.00	15.6	25.73
162	10.7	2477	42.84	153	40.0	8.28	1.09	24.7	25.03
160	11.0	2610	45.90	162	41.7	8.21	1.09	25.0	28.09
158	11.3	2770	49.11	175	43.5	8.19	1.09	25.4	31.68
175	11.6	3223	57.55	184	49.6	8.84	1.18	39.0	33.05
174	11.7	3330	59.44	191	50.8	8.84	1.18	39.2	34.80
172	11.9	3550	63.34	206	53.2	8.83	1.18	40.1	39.19
170	12.2	3760	67.42	221	55.3	8.81	1.18	41.0	44.25
189	12.4	4190	75.74	222	61.1	9.47	1.27	59.9	43.25
187	12.6	4460	80.44	239	63.8	9.47	1.27	60.5	47.55
185	12.9	4720	85.33	256	66.1	9.45	1.27	61.8	53.06
202	13.3	5370	97.92	266	73.6	10.10	1.36	89.9	56.02
201	13.4	5530	100.8	274	75.2	10.10	1.36	90.3	58.45
199	13.6	5850	106.6	294	78.6	10.10	1.36	91.2	63.86
197	13.9	6170	112.6	313	81.0	10.09	1.36	92.3	70.06
215	14.1	6760	124.6	313	88.4	10.72	1.46	131	71.17
213	14.3	7160	131.5	335	92.0	10.73	1.45	132	77.02
211	14.6	7540	138.6	357	94.9	10.73	1.45	133	83.00
209	14.8	7920	145.9	379	98.6	10.71	1.45	135	91.30
236	15.4	9213	172.3	390	112	11.66	1.59	221	97.66
235	15.4	9470	176.7	402	115	11.66	1.59	221	100.7
232	15.6	9980	185.7	428	119	11.67	1.59	223	108.1
230	15.9	10490	194.8	455	123	11.67	1.59	225	116.6
228	16.1	10980	204.3	481	127	11.66	1.59	227	126.0
258	16.6	12280	232.4	476	140	12.60	1.73	357	131.0
255	16.8	12930	243.6	507	145	12.60	1.73	359	139.3
252	17.0	13580	255.0	537	150	12.61	1.73	362	148.7
250	17.2	14220	266.6	568	155	12.61	1.73	364	159.6
277	17.9	16460	313.9	594	175	13.55	1.87	557	176.6
274	18.1	17260	327.9	628	181	13.54	1.87	562	187.9
269	18.5	18860	356.7	700	193	13.53	1.86	576	215.6
263	19.3	21180	402.6	804	209	13.57	1.87	570	252.6

References

Allen, H. G., 1969. *Analysis and Design of Structural Sandwich Construction.* Oxford: Pergamon Press.

ANSYS, 2012. *Online Manuals. Release 12.* [Online].

Bitzer, T., 1994. Honeycomb Marine Applications. *Journal of Reinforced Plastics and Composites,* 13(4), p. 355–360.

Brand, P. R., Whitney, W. S. & Lewis, D. B., 1995. *Load and Resistance Factor Design Case Histories.* Houston, Texas, USA, OTC Offshore Technology Conference, pp. 637-643.

BS 4778, 1991. *Glossary of terms used in quality assurance (including reliability and maintainability terms).* London.

BV, 2022. *MARS 2000 (v. 2.9p).* [Online]
Available at: https://marine-offshore.bureauveritas.com/

Caldwell, J. B., 1965. Ultimate longitudinal strength. *Trans. RINA,* Volume 107, pp. 411-430.

Cornell, A. C., 1969. A probability-based structural code. *ACIJ,* 66(12), pp. 974-985.

Corus Special Profiles, 2002. [Online]
Available at: www.corus-specialprofiles.com
[Accessed 26 February 2022].

De Jong, K. A., 1975. *Analysis of the behaviour of a class of adaptive genetic systems (Doctoral Dissertation),* Ann Arbor: Department of Computer and Communication Sciences, University of Michigan.

Deb, K., Pratap, A., Agarwal, S. & Meyarivan, T., 2002. A fast and elitist multi-objective genetic algorithm: NSGA-II. *IEEE Transactions on Evolutionary Computation,* 6(2), pp. 182-197.

DNV, 1992. *Structural Reliability Analysis of Marine Structures. Classification Notes No. 30.6,* Norway: Det Norske Veritas.

DNV, 2009. *Hull structural design. Ships with length 100 metres above,* Norway: Det Norske Veritas.

DNV, 2010. *Fatigue Assessment of Ship Structures, Classification Notes No 30.7,* Norway: Det Norske Veritas.

DNV, 2021. *Rules for Classification of Ships,* Norway: Det Norske Veritas.

DNV-CG-0128, 2021. *Buckling,* Norway: Det Norske Veritas.

DNV-CG-0154, 2021. *Steel sandwich panel construction,* Norway: Det Norske Veritas.

Dorigo, M., Maniezzo, V. & Colorni, A., 1991. *Positive feedback as a search strategy. Tech. Rep. 91-016,* Milano: Dipartimento di Elettronica, Politecnico di Milano, Italy.

Edgeworth, F. Y., 1881. *Mathematical Psychics, an essay on applying mathematics to the moral sciences, by F.Y. Edgeworth.* London: C.K. Paul.

Evans, J. H., 1959. Basic Design Concepts. *Journal of the American Society for Naval Architects,* 71(4), pp. 671-678.

Evans, J. & Khoushy, D., 1963. Optimised Design of Midship Section Structure. *Trans. SNAME,* Issue 71, pp. 144-191.

Feng, G., Dongsheng, W., Garbatov, Y. & Guedes Soares, C., 2015. Reliability Analysis Based on a Direct Ship Hull Strength Assessment. *Journal of Marine Science and Application,* 14(04), pp. 389-398.

Feng, Y., Qiu, H., Gao, Y. & Zheng, H., 2020. Creative design for sandwich structures: a review. *International Journal of Advances Robotic Systems,* 17(3), pp. 1-24.

Garbatov, Y. & Georgiev, P., 2017. Optimal design of stiffened plate subjected to combined stochastic loads. In: *Progress in the Analysis and Design of Marine Structures.* London: Taylor & Francis Group, pp. 243-252.

Garbatov, Y., Scattareggia Marchese, S., Palomba, G. & Crupi, V., 2022. Alternative hybrid lightweight ship hull structural design. In: C. Guedes Soares & T. Santos, eds. *Trends in Maritime Technology and Engineering.* London: CRC Press, pp. 99-107.

Garbatov, Y., Sisci, F. & Ventura, M., 2018. Risk-based framework for ship and structural design accounting for maintenance planning. *Ocean Engineering,* Volume 166, pp. 12-25.

Glover, F. & Laguna, M., 1997. *Tabu search.* New York: Kluwer Academic Publishers.

Goldberg, D. E., 1983. *Computer-aided gas pipeline operation using genetic algorithms and rule learning (Doctoral Dissertation).* 3174B ed. Ann Arbor: University of Michigan.

Goldberg, D. E., 1989. *Genetic algorithms in search, optimisation and machine learning.* Reading, NY: Addison-Wesley.

Guedes Soares, C., 1990. Stochastic Modelling of Maximum Still-Water Load Effects in Ship Structures. *Journal of Ship Research,* Volume 34, pp. 199-205.

Guedes Soares, C. et al., 1996. Reliability-Based Ship Structural Design. *Trans. SNAME,* Volume 104, pp. 359-389.

Guedes Soares, C. & Moan, T., 1988. Statistical Analysis of Still-Water Load Effects in Ship Structures. *Trans. SNAME,* Volume 96, pp. 129-156.

Guedes Soares, C. & Teixeira, A. P., 2001. Risk assessment in maritime transportation. *Reliability Engineering & System Safety,* 74(3), pp. 299-309.

Harlander, L., 1960. Optimum Plate-Stiffener Arrangement for Various Types of Loading. *Journal of Ship Research,* 4(20), pp. 49-65.

Hasofer, A. M. & Lind, N. C., 1974. An exact and invariant first-order reliability format. *Journal of Engineering Mechanics Division,* Volume 100, pp. 111-121.

Hentinen, M., Hildebrand, M. & Visuri, M., 1997. *Adhesively bonded joints between FRP sandwich and metal: different concepts and their strength behaviour.* s.l.:VTT Tiedotteita - Valtion Teknillinen Tutkimuskeskus.

HexCel Composites, 2000. *HexWeb Honeycomb Sandwich Design Technology.* [Online] [Accessed 2022].

Holland, J. H., 1975. *Adaptation in natural and artificial systems: An introductory analysis with applications to biology, control, and artificial intelligence.* Ann Arbor, Michigan, USA: University of Michigan Press.

Huang, Y. C. & Garbatov, Y., 2020. Multi-objective Reliability-Based Design of Ship Structures Subjected to Fatigue Damage and Compressive Collapse. *Journal of Offshore Mechanics and Arctic Engineering,* Volume 142(5), pp. 051701-1 - 051701-6.

Hughes, O. F. & Paik, J. K., 2010. *Ship Structural Design and Analysis.* New Jersey: The Society of Naval Architects and Marine Engineers.

Hughes, O., Ma, M. & Paik, J. K., 2014. *Applications of Vector Evaluated Genetic Algorithms (VEGA) in Ultimate Limit State Based Ship Structural Design.* San Francisco, California, USA, pp. 1-9.

Hughes, O., Mistree, F. & Zanic, V., 1980. A Practical Method for the Rational Design of Ship Structures. *Journal of Ship Research,* 24(2), pp. 101-113.

IACS, 2021. *Common Structural Rules for Bulk Carriers and Oil Tankers.*

IMO, 1966. *International Convention on Load Lines,* London.

IMO, 1993. *International Management Code for the Safe Operation of Ships and for Pollution Prevention (International Safety Management (ISM) Code). Resolution A.741(18),* London.

IMO, 1997. *Interim Guidelines for the Application of Formal Safety Assessment (FSA) to the IMO Rule-Making Process, MSC/Circ. 829 (MEPC/Circ. 335),* London.

IMO, 2002. *Guidelines for Formal Safety Assessment (FSA) for Use in the IMO Rule-Making Process. MSC/Circ.1023, MEPC/Circ.392,* London.

IMO, 2006. *FSA-Report of the Correspondence group MSC 81/18,* London.

IMO, 2008. *Formal safety assessment on crude oil tankers,* London.

IMO, 2009. *Hong Kong International Convention for the Safe and Environmentally Sound Recycling of Ships.*

IMO, 2011. *Resolution MEPC.203(62),* London.

IMO, 2013. *Revised guidelines for formal safety assessment (FSA) for use in the IMO rule-making process. MSC-MEPC.2/Circ.12.* London.

IMO, 2018. *Revised Guidelines for Formal Safety Assessment (FSA) for Use in the IMO Rule-Making Process. MSC-MEPC.2/Circ.12/Rev.2.* London.

ISO 8402, 1994. *International Standards Organization.*

ISSC, 2003. *Committee III.1 – Ultimate Strength.* San Diego: International Ship and Offshore Structures Congress.

Jastrzebski, T. & Sekulski, Z., 2005. Application of genetic algorithm to structural optimisation of high speed craft. In: *Maritime Transportation and Exploitation of Ocean and Coastal Resources.* London, UK: Taylor & Francis Group, pp. 859-866.

Katoch, S., Chauhan, S. & Kumar, V., 2021. A review on genetic algorithm: past, present, and future. *Multimedia Tools and Applications,* Volume 80, pp. 8091-8126.

Kelsey, S., Gellatly, R. A. & Clark, B. W., 1958. The Shear Modulus of Foil Honeycomb Cores. *Aircraft Engineering and Aerospace Technology,* 30(10), pp. 294-302.

Kennedy, J. & Eberhart, R., 1995. *Particle Swarm Optimization.* Perth, Australia, pp. 1942-1948.

Kharghani, N. & Guedes Soares, C., 2018. Experimental and numerical study of hybrid steel-FRP balcony overhang of ships under shear and bending. *Marine Structures,* Volume 60, pp. 15-33.

Kirpatrick, S., Gelatt, C. D. & Vecchi, M. P., 1983. Optimisation by simulated annealing. *Science,* 220(4598), pp. 671-680.

Klanac, A. & Jelovica, J., 2007. *A concept of omni-optimization for ship structural design.* Glasgow, UK, Advancements in Marine Structures - Proceedings of MARSTRUCT 2007, The 1st International Conference on Marine Structures, pp. 473-482.

Kobayashi, H., Daimaruya, M. & Okuto, K., 1994. Elasto-Plastic Bending Deformation of Welded Honeycomb Sandwich Panel. *JSME International Journal,* 60(572), pp. 1011-1016.

Kujala, P. & Klanac, A., 2005. Steel Sandwich Panels in Marine Applications. *Brodogradnja: Teorija i praksa brodogradnje i pomorske tehnike,* 56(4), pp. 305-314.

Made in China, 2022. *www.made-in-china.com.* [Online]
[Accessed July 2022].

MAESTRO Marine LLC Software, v11.2. [Online]
Available at: https://www.maestromarine.com/

Mahfoud, M. & Emade, D., 2010. Aluminium Recycling - Challenges and Opportunities. *Advanced Materials Research,* Volume 83.86, pp. 571-578.

Ma, M., Hughes, O. & McNatt, T., 2015. *Ultimate Limit State-Based Ship Structural Design Using Multi-Objective Discrete Particle Swarm Optimization.* St. John's, Newfoundland, Canada, pp. 1-10.

MARPOL, 1973. *International Convention for the Prevention of Pollution from Ships (MARPOL 73/78).* London.

MSA, 1993. *Formal safety assessment MSC66/14, Submitted by the United Kingdom to IMO Maritime Safety Committee.*

Nepomuceno de Oliveira, M. A., Szklo, A. & Castelo Branco, D. A., 2022. Implementation of Maritime Transport Mitigation Measures according to their marginal abatement costs and their mitigation potentials. *Energy Policy,* Volume 160, p. 112699.

Nobuwaka, H. & Zhou, G., 1996. Discrete Optimisation of Ship Structures with Genetic Algorithms. *Journal of The Society of Naval Architects of Japan,* Volume 179, pp. 293-301.

Nowacki, H., Brusis, F. & Swift, P., 1970. Tanker Preliminary design – An Optimisation Problem with Constraints. *Trans. SNAME,* Issue 78, pp. 357-390.

Okada, T. & Neki, I., 1992. Utilisation of genetic algorithm for optimising the design of ship hull structures. *Journal of The Society of Naval Architects of Japan 171,* pp. 71-83.

Okuto, K., Namba, K., Mizukoshi, H. & Hiyama, Y., 1991. The analysis and design of honeycomb welded structure. *J Light Met Welding,* 29(8), pp. 361-8.

Paik, J. K., 2003. ALPS/HULL User's Manual, A Computer Program for the Progressive Collapse Analysis of Ship Hulls. *Ship Structural Mechanics Laboratory.*

Paik, J. K. & Mansour, A. E., 1995. A simple formulation for predicting the ultimate strength of ships. *Marine Science and Technology,* Volume 1, pp. 52-62.

Paik, J. K., Thayamballi, A. K. & Gyu Sung, K., 1999. The strength characteristics of aluminium honeycomb sandwich panels. *Thin-Walled Structures,* Volume 35, pp. 205-231.

Palaversa, M., Prebeg, P. & Andric, J., 2020. Current State of Development of Ship Structural Design and Optimisation Methods. *Journal of Maritime & Transportation Science,* 3(3), pp. 171-187.

Palomba, G., Epasto, G., Sutherland, L. & Crupi, V., 2021. Aluminium honeycomb sandwich as a design alternative for lightweight marine structures. *Ships and Offshore Structures,* pp. 1-12.

Papanikolaou, A. & Konovessis, D., 1999. *Safety in Ship Design: Review of Fundamental Concepts and Methodologies.* Glasgow, UK, pp. 23-42.

Pareto, V., 1906. *Manuale di economia politica: con una introduzionea alla scienza sociale.* Milano: Società Editrice Libraria.

Parsons, M. G. & Scott, R. L., 2004. Formulation of Multi criterion Design Optimisation Problems for Solutions with Scalar Numerical Optimization Methods. *Journal of Ship Research,* 48(1), pp. 61-76.

Parunov, J., Andric, J. C. M. & Kitarovic, S., 2015. Structural reliability assessment of container ship at the time of accident. *Journal of Engineering for the Maritime Environment,* 229(2), pp. 111-123.

Parunov, J. & Guedes Soares, G., 2008. Effects of Common Structural Rules on hull-girder reliability of an Aframax oil tanker. *Reliability Engineering and System Safety,* Volume 93, pp. 1317-1327.

Plantema, F. J., 1966. *Sandwich Construction.* New York: Pergamon Press.

Qin, Z. & Batra, R. C., 2009. Local slamming impact of composite sandwich hulls. *International Journal of Solids and Structures,* Volume 46, pp. 2011-2035.

Rackwitz, R. & Fiessler, B., 1978. Structural Reliability under Combined Random Load Sequences Computers and Structures. *Computers and Structures,* 9(5), pp. 489-494.

Rausand, M., 1998. Introduction to Reliability Engineering. In: *Risk and Reliability in Marine Technology.* Rotterdam, NL: Balkema, pp. 371-381.

Rigo, P., 2001. A module-oriented tool for optimum design of stiffened structures – Part I. *Marine Structures,* Volume 14, pp. 611-629.

Rigo, P., 2003. An Integrated Software for Scantling Optimization and Least Production Cost. *Ship Technology Research,* 50(3), pp. 125-140.

Schaffer, J. D., 1985. *Multi-objective optimisation with vector-evaluated genetic algorithms.* Hillsdale, New Jersey, Lawrence Erlbaun Associates, pp. 93-100.

Sharma, S., Rangaiah, G. P. & Cheah, K. S., 2012. Multi-objective optimisation using MS Excel with an Application to Design of a Falling-film Evaporator System. *Food and Bioproducts Processing,* 90(2), pp. 123-134.

Sharma, S., Rangaiah, G. P. & Cheah, K. S., 2012. Multi-objective optimisation using MS Excel with an Application to Design of a Falling-film Evaporator System. *Food and Bioproducts Processing,* 90(2), pp. 123-134.

Sharma, S., Rangaiah, G. P. & Marechal, F., 2017. Multi-objective optimisation Programs and Their Application to Amine Absorption Process Design for Natural Gas Sweetening. In: G. P. Rangaiah, ed. *Multi-objective*

optimisation: Techniques and Application in Chemical Engineering. Singapore: World Scientific, pp. 533-560.

Smith, C., 1977. *Influence of Local Compressive Failure on Ultimate Longitudinal Strength of a Ship Hull.* Tokyo, JPN, pp. 73-79.

SOLAS, 1914-1974. *International Convention for the Safety of Life at Sea.* London.

Spouge, J., 1989. The Safety of Ro-Ro Passenger Ferries. *Trans. SNAME,* Volume 131.

Srinivas, N., Deb, K. & Deb, K., 1994. Multi-objective Optimisation Using Nondominated Sorting in Genetic Algorithms. *Evolutionary Computation,* 2(3), pp. 221-248.

Teixeira, A. P. & Guedes Soares, C., 2005. *Assessment of partial safety factors for the longitudinal strength of tankers.* Lisbon, Francis and Taylor, pp. 1601-1610.

Teixeira, A. P. & Guedes Soares, C., 2007a. Economical and social criteria for risk acceptance. In: *Public and Industrial Risks (in Portuguese).* Lisbon, Portugal: Edições Salamandra, Lda., pp. 45-63.

Teixeira, A. P. & Guedes Soares, C., 2007b. Economical considerations in establishing an optimal safety level for structures. In: *Public and Industrial Risks (in Portuguese).* Lisbon, Portugal: Edições Salamandra, Lda., pp. 623-642.

Tekgoz, M. & Garbatov, Y., 2020. Strength Assessment of Rectangular Plates Subjected to Extreme Cyclic Load Reversals. *Journal of Marine Science and Engineering,* 8(2), pp. 1-21.

Tekgoz, M. & Garbatov, Y., 2021. Collapse Strength of Intact Ship Structures. *Journal of Marine Science and Engineering,* 9(10), p. 1079.

Tekgoz, M., Garbatov, Y. & Guedes Soares, C., 2015. Ultimate strength assessment of a container ship accounting for the effect of neutral axis movement. In: *Maritime Technology and Engineering.* London, UK: Taylor & Francis Group, pp. 417-423.

Ueda, Y. & Rashed, M. H., 1984. The Idealised Structural Unit Method and its Application to Deep Girder Structures. *Computers and Structures,* 18(2), pp. 277-293.

United Nations, 1948. *Convention on the International Maritime Organization.* Geneva.

Vinson, J. R., 1999. *The behaviour of sandwich structures of isotropic and composite materials.* Lancaster, Pennsylvania: Technomic.

Wang, J., 1994. *Formal safety analysis methods and their application to the design process.* UK: University of Newcastle Upon Tyne.

Wang, J., 2006. Maritime Risk Assessment and its Current Status. *Quality and Reliability Engineering International,* 22(1), pp. 3-19.

Wang, J. et al., 2004. Use of Advances in Technology for Maritime Risk Assessment. *Risk Analysis,* 24(4), pp. 1041-1063.

Wang, J., Yang, J. B., Sen, P. & Ruxton, T., 1996. Safety ased design and maintenance optimisation of large marine engineering systems. *Applied Ocean Research,* 18(1), pp. 13-27.

Wong, J. Y. Q., Sharma, S. & Rangaiah, G. P., 2016. Design of Shell-and-Tube Heat Exchangers for Multiple Objectives Using Elitist Non-dominated Sorting Genetic Algorithm with Termination Criteria. *Applied Thermal Engineering,* Volume 93, pp. 888-899.

Yeh, W. N. & Wu, Y. E., 1991. Enhancement of buckling characteristics for sandwich structure with fibre-reinforced composite skins and core made of aluminium honeycomb and polyurethane foam. *Theoretical and Applied Fracture Mechanics,* Volume 15, pp. 63-74.

Zenkert, D., 1993. *An Introduction to Sandwich Construction.* Department of Lightweight Structures, Royal Institute of Technology.

Zenkert, D., Shipsha, A., Bull, P. & Hayman, B., 2005. Damage tolerance assessment of composite sandwich panels with localised damage. *Composites Science And Technology,* 65(15-16), pp. 2597-2611.